



EUROPEAN COMMISSION  
JOINT RESEARCH CENTRE

Institute for Environment and Sustainability  
Inland and Marine Waters Unit  
I-21020 Ispra (VA) Italy

# **Application of the Divergence Criterion to Isoperibolic Batch Reactors: Simulated and Experimental Results**

**AWARD Project (Advanced Warning And Runaway Disposal)**  
(Growth Project G1RD-CT-2000-00499)

***J. Bosch, F. Strozzi***  
Carlo Cattaneo University  
Quantitative Methods Institute  
Castellanza (VA) Italy

***J. Zbilut***  
Department of Molecular Biophysics and Physiology  
Rush University, Chicago – USA

***J.M. Zaldivar***

**Mission:**

The mission of the Institute for Environment and Sustainability is to provide scientific and technical support to EU strategies for the protection of the environment and sustainable development. Employing an integrated approach to the investigation of air, water and soil contaminants, its goals are sustainable management of water resources, protection and maintenance of drinking waters, good functioning of aquatic ecosystems, and good ecological quality of surface waters.

**LEGAL NOTICE**

Neither the European Commission nor any person acting on behalf of the Commission is responsible for the use which might be made of the following information.

A great deal of additional information on the European Union is available on the Internet. It can be accessed through the Europa server (<http://europa.eu.int>)

EUR 20388 EN

© European Communities, 2002

Reproduction is authorised provided the source is acknowledged

*Printed in Italy*

# CONTENTS

## 1. INTRODUCTION

## 2. STATE SPACE RECONSTRUCTION

2.1. Embedding parameters

2.2. Time delayed vectors, derivatives and integral coordinates

## 3. DIVERGENCE CALCULATION

3.1. Volume (Area) calculation

3.2. Jacobian reconstruction

## 4. RUNAWAY DETECTION USING SIMULATED DATA

4.1. Preliminary analysis using all state variables

4.2. Physical interpretation of the numerical divergence criterion as a function of the embedding dimension

4.3. Reconstruction using time delay vectors, derivatives and integrals

## 5. RUNAWAY DETECTION USING EXPERIMENTAL DATA

5.1. Description of the experimental data sets

5.2. Nonlinear noise reduction

5.3. Runaway detection

## 6. CONCLUSIONS AND FUTURE WORK

**Appendix 1. Relationship between the Jacobian in continuous and discrete systems**

**NOTATION**

**REFERENCES**



**AWARD (Advanced Warning And Runaway Disposal) Project**  
(Growth Project G1RD-CT-2000-00499)

**Deliverable:** Advancement report on the improvement and testing of state space reconstruction numerical schemes (**WP2.Extension and theoretical development of the EWDS**. Task 2.2, First Part: Batch and Semibatch reactors working on isoperibolic operating conditions)

**Objective:** The objective of Task 2.2 is to implement and test several reconstruction algorithms to be used for the on-line reconstruction of the divergence of the system, using simulation results from Task 2.1 and experimental results from WP 4 (Task 4.1).

### **Summary**

In this work, we have demonstrated that the application on-line of the divergence criterion for the early warning detection of runaway initiation is feasible. Furthermore, we have shown the equivalence, considering an embedding dimension of one, between Hub and Jones (1987) and  $div > 0$  criteria. The use of an embedding dimension of two can be seen as a way to solve the problem of false alarms that the Hub and Jones criterion produces, for example for the case of autocatalytic reactions.

Theoretical results have shown that the best results are obtained by considering three temperature trajectories to calculate the evolution of the state space volume. However, experimentally it seems that only one temperature would produce better results. This is due to the fluctuation and noise present in the system, and further research using different experiments and different reactors is necessary to assess which is the best procedure. Of course, from the practical point of view, the use of only one temperature measurement would simplify considerably the real application of the early warning detection device.

In order to develop a robust early warning detection system it is now necessary to study the reconstruction in the case of controlled jacket temperature in which the dynamics of the heating/cooling circuits plus the control system have to be taken into account and, finally, to show their feasibility in "realistic" situations, i.e. in industrial plants under normal and abnormal operating conditions. Our research is continuing along these lines.



## 1. INTRODUCTION

Safety improvements at the level of a particular chemical process can only be achieved through the long process of research and engineering experience. Nevertheless, despite conventional fall-back mechanisms, switches and multi-layer control circuitry available today, there is always the possibility of undetected runaway events. A safe reactor is therefore not only characterised by the degree of the complexity of its safety measures but also by the rate with which unexpected and unavoidable potentially dangerous situations can be handled. Early warning devices are therefore indispensable, irrespective of the detailed mechanisms of the reaction and of other safety measures.

Normally, an early warning detection system consists of the following parts (Isermann, 1994): interface with the process to acquire data (monitoring); criteria to distinguish between dangerous situations and non-dangerous ones (detection); procedure for triggering off the alarms (diagnosis and evaluation). After the detection system has found an alarm in the process, the decision about the counter-measures to be adopted has to be made.

In a series of recent works (Strozzi *et al.*, 1999; Zaldívar *et al.*, 2002) a new criterion to delimit runaway boundaries was developed using techniques from chaos theory and the fact that the sensitivity to initial and operating conditions is a well-known characteristic of chemical reactors (Varma *et al.*, 1999). According to the analysis and previous criteria, the early warning detection criterion was defined as when the divergence of the batch or semibatch reactor becomes positive on a segment of the reaction path, i.e.  $div > 0$ . We recall that the divergence is a scalar quantity defined at each point as the sum of the partial derivatives of the mass and energy balances with relation to the correspondent variables -temperature and conversions-, i.e.,  $\partial(dT/dt)/\partial T + \sum_i \partial(dz_i/dt)/\partial z_i$ .

This criterion was compared with previous ones. The results show its validity even in the case of autocatalytic reactions, where previous criteria (Adler and Enig, 1964; Hub and Jones, 1986) were unable to define a suitable boundary for runaway characterisation. Furthermore, its has recently been extended to other type of reactions, i.e. parallel, consecutive, polymerisations, etc., other type of reactors, i.e. BR, SBR and CSTR, and different operating conditions, i.e. isoperibolic – constant jacket temperature- and isothermal –with controlled jacket temperature (Zaldívar *et al.*, 2002).

It was then shown, from a theoretical analysis using simulated data, that the divergence of the system could be reconstructed from only temperature measurements (Strozzi *et al.*, 1999) and that by measuring several temperatures inside the reactor one could do the same experimentally. However, the procedure was not sufficiently robust against noise in temperature measurements for the pilot plant (100 L) reactor experiments (Strozzi *et al.*, 1998). An improvement using a related

technique, i.e. Recurrence Quantification Analysis (RQA), has been recently developed (Zbilut *et al.*, 2002) in which only one temperature measurement is needed and which is robust against noise contamination. However, despite the fact that there is a relation between the values obtained in the RQA and the divergence of the system, it is difficult to quantify this relation. Hence, in order to continue the development of the divergence criterion, and the related early warning detection system for runaway initiation, we have studied several alternatives to reconstruct the state space from only temperature measurements, how to calculate the divergence in these reconstructed state spaces and how to increase the robustness against noise.

First, several cases have been studied using simulated data and subsequently experimental data from bench scale reactors and pilot plant installations has been analysed. The results show that the criterion is able to detect the runaway initiation even in the presence of noise and fluctuations. Several strategies have been implemented but further experiments are necessary to decide which is the more robust alternative.

The work has been divided as follows, in Section 2 we introduce state space reconstruction and the different techniques, whereas in Section 3 the calculation of divergence in the reconstructed state space is shown. After this theoretical introduction, Section 4 is devoted to the results obtained using simulated data that has been studied in Zaldívar *et al.* (2002) to assess the validity of the divergence criterion. The study using data from isoperibolic batch and semibatch experiments carried out in a bench-scale reactor (2 L) and in a pilot plant reactor (100 L) is presented in Section 5 where several noise reduction techniques are discussed and the early warning detection results are presented. Finally, in Section 6, we made some conclusions and describe future work.

## **2. STATE SPACE RECONSTRUCTION**

A useful idea from non-linear systems theory is the theory of embedding. The theory of embedding is a way to move from a temporal time series of measurements to a state space "similar" -in a topological sense- to that of the underlying dynamical system we are interested in analysing. Techniques of state space reconstruction were introduced by Packard *et al.* (1980) and Takens (1981), which showed, under certain generic assumptions, that it is possible to address this problem using measurements of a time series of the dynamical system of interest.

In order to understand the relationship that occurs between the space of measurements and the real state space, let us consider the two consecutive reactions in an isoperibolic batch reactor system:

$$\frac{du_A}{dt} = -f_1 u_A^{n_1} \quad (1)$$

$$\frac{du_B}{dt} = f_1 u_A^{n_1} - \rho f_2 u_B^{n_2} \quad (2)$$

$$\frac{d\theta}{dt} = \alpha f_1 u_A^{n_1} + \alpha \lambda \rho f_2 u_B^{n_2} - \beta(\theta - 1) \quad (3)$$

The reactions are assumed to be  $n_i$ -th order with respect to reactant and to follow Arrhenius temperature dependence, i.e.  $f_i = \exp[\gamma_i(\theta - 1)/\theta]$ .  $\rho$  and  $\lambda$  are the reaction rate constant ratio and the heat of reaction ratio ( $\Delta H_2/\Delta H_1$ ), respectively; whereas  $\alpha$  and  $\beta$  are the dimensionless heat of reaction and dimensionless heat transfer parameters (see Notation for a complete definition of all variables and parameters).

We can define  $\mathbf{y} = (y_1, y_2, y_3)$  as follows:  $\mathbf{y} = (\theta, d\theta/dt, d^2\theta/dt^2)$ , then the equations of motion take the form:

$$\frac{dy_1}{dt} = y_2 \quad (4)$$

$$\frac{dy_2}{dt} = y_3 \quad (5)$$

$$\frac{dy_3}{dt} = \mathbf{G}(y_1, y_2, y_3) \quad (6)$$

for some function  $\mathbf{G}$ . In this coordinate system, modelling the dynamics reduces to constructing the single function  $\mathbf{G}$  of three variables, rather than three separate functions, each of three variables.

In this way we may proceed from the state space  $(u_A, u_B, \theta)$  to the space of derivatives  $\{\theta, d\theta/dt, d^2\theta/dt^2\}$ . The dynamics in this new space will be related to the dynamics of the original space by a nonlinear transformation, which is called the reconstruction map. The extension of this approach to higher-dimensional dynamical systems is straightforward by considering higher derivatives.

Takens (1981) showed that instead of derivatives, one can use delay coordinates,  $\{\theta(t), \theta(t-\Delta t), \theta(t-2\Delta t)\}$ , where  $\Delta t$  is a suitably chosen time delay. In fact, looking at the following approximation of the derivative of  $\theta(t)$ :

$$\frac{d\theta(t)}{dt} \cong \frac{\theta(t + \Delta t) - \theta(t)}{\Delta t} \quad (7)$$

$$\frac{d^2\theta(t)}{dt^2} \cong \frac{\theta(t + 2\Delta t) - 2\theta(t + \Delta t) - \theta(t)}{2\Delta t^2} \quad (8)$$

it is clear that the new information brought from every new derivative is contained in the series of the delay coordinates. The advantage of using delay coordinates instead of derivatives is that in case of high dimensions high order derivatives will tend to amplify considerably the noise in the measurements.

In a general case, let  $s(t)$  be the measure of some variable of our system, which is related to the state variables by an unknown function  $h$ ,

$$s(t) = h(\mathbf{x}(t)) \quad (9)$$

Takens (1981) proved that, under certain conditions, the dynamics on the attractor of the underlying original system has a one-to-one correspondence with measurements of a limited number of variables.

This observation opened a new field of research: nonlinear time series analysis (Abarbanel, 1996; Kantz and Schreiber, 1997; Diks, 1999). In fact, if the equations defining the underlying dynamical system are not known, and we are not able to measure all the state space variables, the state space of the original system is not directly accessible to us. However, if by measuring few variables we are able to reconstruct a one-to-one correspondence between the reconstructed state space and the original, this means that it is possible to identify unambiguously the original state space from measurements. But what kind of information about the original space is preserved in the new one?

There are two types of preserved information: qualitative and quantitative. Qualitative information is that which allows a qualitative description of the dynamics described by topological invariants, such as singularity of the field, closeness of an orbit, stability of a fixed point, etc. Quantitative information can be of two different types: geometrical and dynamical. Geometrical methods depend on the computation of various fractal dimensions or scaling functions. Dynamical methods rely on the estimation of local and global Lyapunov exponents and Lyapunov dimension. Concerning the case of chemical reactors, we are interested in reconstructing the divergence of the system. This quantity is, in principle, preserved under state space reconstruction as was shown by Strozzi (1997).

## 2.1. Embedding parameters

There are two parameters we need to calculate to reconstruct the state space using delay coordinates,  $\{s(t), s(t-\Delta t), s(t-2\Delta t), \dots, s(t-(d_E-1)\Delta t)\}$ : the time delay,  $\Delta t$ , and the embedding dimension,  $d_E$ , whereas for the case of derivatives,  $\{s(t), ds(t)/dt, \dots, d^{(d_E-1)}s(t)/dt^{(d_E-1)}\}$ , there is no need to determine an optimum time delay.

The embedding dimension is the dimension we need to unfold the underlying dynamics of our system. Working in a dimension larger than the minimum required by the data will lead to excessive requirements in terms of the number of data points and computation times necessary when investigating different questions such as, for example invariants calculation (the divergence in our case). Furthermore, noise by definition has an infinite embedding dimension, so it will tend to occupy the additional dimensions of the embedding space where no real dynamics is operating and, hence, it will increase the error in the subsequent calculations. On the other hand, by selecting an embedding dimension lower than required, we would not be able to unfold the underlying dynamics, i.e. the calculations would be wrong since we do not have an embedding. Similar problems can be found when choosing the time delay. If the time delay chosen is too small, there is almost no difference between the elements of the delay vectors, since that all points are accumulated around the bisectrix of the embedding space: this is called redundancy. However, when  $\Delta t$  is very large, the different co-ordinates may be almost uncorrelated. In this case the reconstructed attractor may become very complicated, even if the underlying "true" attractor is simple: this is called irrelevance. Unfortunately no rigorous way exists of determining the optimal value of  $\Delta t$ .

In relation with the concept of embedding dimension, it is necessary to say that in the case of the so-called dissipative systems, the flow will contract onto sets of lower dimension, which are called attractors. On the attractor the system has fewer degrees of freedom and consequently requires less information to specify its state. For example, in the case of consecutive reactions the state space has dimension 3, see Eqs. (1)-(3). However, the final attractor, when all reactants have been depleted and the reactor temperature is equal to the jacket temperature, is a fixed point and hence it has a dimension of 0. However, we are not interested in studying the fixed point or final attractor of our system, we are interested in studying the transient dynamics, and although there have been numerous proposals for the choice of time delay (Mees *et al.*, 1987; Fraser and Swinney, 1986, amongst others) and for the selection of the embedding dimension (Kennel *et al.*, 1992; Cao, 1997, a.o.), they all are presented with the assumption of stationarity, which in our case does not hold.

In the context of nonstationarity, the notion of a "correct" embedding or delay is inappropriate as has been demonstrated by Grassberger *et al.* (1991). Instead it becomes important to remember that a sufficiently large embedding be chosen which will "contain" the relevant dynamics (as it may change from one dimensionality to another) as well as account the effects of noise, which tend to inflate dimension. Hegger *et al.* (2000) have justified the approach to "overembed" the time series to capture the dynamics as its dimension changes. Similar considerations govern the choice of the time delay. As the system changes from one dimension to another the effects of the time delay are

performance changed. Thus a so-called “optimal” time delay in one embedding, becomes less so as the relevant dimension changes (Zbilut *et al.*, 2002).

## 2.2. Time delayed vectors, derivatives and integral coordinates

Unfortunately, there is no rigorous way of determining which will be the best state space reconstruction method. In this work we have tested several methods to determine an optimal reconstruction for our system. The following methods has been analysed: time delay embedding vector:  $\{s(t), s(t-\Delta t), s(t-2\Delta t), \dots, s(t-(d_E-1)\Delta t)\}$ ; derivative coordinates,  $\{s(t), ds(t)/dt, \dots, d^{(d_E-1)}s(t)/dt^{(d_E-1)}\}$  and integral coordinates,  $\{s(t), I_1[s(t)], \dots, I_{d_E-1}[s(t)]\}$ .

As stated before for time delay embedding vectors we need to define a time delay and an embedding dimension. Time delayed vectors are the most used reconstruction method for chaotic attractors since small amount of noise tend to corrupt algorithms to calculate the invariant properties, for example, fractal dimension, Lyapunov exponents, etc.

The advantage of derivative coordinates,  $\{s(t), ds(t)/dt, \dots, d^{(d_E-1)}s(t)/dt^{(d_E-1)}\}$ , is their clear physical meaning, as has been already introduced; their drawback lies in their sensitivity to noise. In fact as it has been shown in Kantz and Schreiber (1997) the first derivative is corrupted by a much larger noise level than the signal itself, and the noise level increases at higher derivatives. For this reason, derivative coordinates are to be used with care, and using low-pass filtered data. Otherwise, state space reconstruction will not be possible. Furthermore, there are several methods to approximate the derivatives of a time series. For example using three points it is possible to obtain several approximations to the first derivative (Burden and Faires, 1985):  $\dot{s}(t) \approx [-3s(t) + 4s(t+h) - s(t+2h)]/2h$ ,  $\dot{s}(t) \approx [-s(t) + s(t+h)]/2h$ , and  $\dot{s}(t) \approx [s(t-2h) - 4s(t-h) + 3s(t)]/2h$ . This will give slightly different embeddings, so there is not only one method. Of course, for noise free data, the more accurate method will produce the best results. However, in the case of noisy signals this is not guaranteed.

Instead of derivatives it might also be reasonable to introduce integrals of the signal (Kantz and Schreiber, 1997), for example:

$$I_1[s(t)] = \int_0^t s(\tau) d\tau, \quad (10)$$

or to use a mixed representation. Also in this case depending on the numerical method used to calculate the integrals we will obtain different embeddings.

### 3. DIVERGENCE CALCULATION

The phase space reconstruction theory has been developed for studying the attractor that will be reached by our system, i.e. the long time behaviour of the system. However, in the case of batch and semibatch reactors, the final attractor is a fixed point, i.e. when all reactants have been depleted and the reactor temperature is in equilibrium with the jacket temperature, which has not so much interest. In these reactors, the interesting region in which we are trying to reconstruct the system is the transient region. In this sense, we are applying chaos theory techniques out of the context they were developed for, so special care has to be taken, since there is no guarantee they will work out.

Let us consider a system of  $n$  ordinary differential equations, in our case energy and mass balances, defined as:

$$\frac{d\mathbf{x}(t)}{dt} = \mathbf{F}(\mathbf{x}(t)) \quad (11)$$

where  $\mathbf{x}(t)=[x_1(t), x_2(t), \dots, x_n(t)]$  in  $\mathbb{R}^n$  and  $\mathbf{F}=[F_1, \dots, F_n]$  is a smooth nonlinear function of  $\mathbf{x}$ , i.e. that the existence and uniqueness properties hold. At time  $t > 0$  the initial condition  $\mathbf{x}(0)$  finds itself at some new point  $\mathbf{x}(t)$ . Similarly, all initial conditions lying in a certain region  $I(0)$  find themselves in another region  $I(t)$  after time  $t$ . If we let  $V(t)$  denote the volume of the region  $I(t)$ , then a strong version of Liouville's theorem (Arnold, 1973) states that:

$$\frac{dV(t)}{dt} = \int_{\Gamma(t)} \text{tr}[J(x)] dx_1 \dots dx_n \quad (12)$$

where

$$\text{div}[J(x)] = \frac{\partial F_1(x)}{\partial x_1} + \dots + \frac{\partial F_n(x)}{\partial x_n} \quad (13)$$

Assuming that our  $n$ -dimensional volume is small enough that the divergence of the vector field is constant over  $V(t)$ , then

$$\frac{dV(t)}{dt} = V(t) \cdot \text{div}[J(x)] \quad (14)$$

and hence,

$$\int_0^t \frac{dV(\tau)}{V(\tau)} = \int_0^t \text{div}[J(x)] d\tau \quad (15)$$

which means that the initial phase space volume  $V(0)$  shrinks (grows) with time in  $\mathbb{R}^n$  as:

$$V(t) = V(0) \cdot \exp \left[ \int_0^t \text{div}[J(x)] d\tau \right] \quad (16)$$

Hence, for the case of a system given by Eq. (11), the rate of change of an infinitesimal volume  $V(t)$  following an orbit  $x(t)$  is given by the divergence of the flow which is locally equivalent to the trace of the Jacobian. The integral of a strictly positive (negative) function is itself strictly positive (negative), and the integral of an identically zero function is identically zero. That means if  $\text{div}[\mathbf{F}(\mathbf{x})] < 0 \forall \mathbf{x}$  in the state space then the flow of trajectories is volume-contracting, if  $\text{div}[\mathbf{F}(\mathbf{x})] > 0 \forall \mathbf{x}$  the flow is volume-expanding, and if  $\text{div}[\mathbf{F}(\mathbf{x})]=0 \forall \mathbf{x}$  then the flow is volume-preserving.

There are several methods to calculate numerically the divergence of a system. In principle the results should be equivalent, but due to numerical truncation errors there are several differences in the numerical results as we will see later on. However, all these methods are based on the general principle that we have a set of nearby trajectories and that between this set we select the closest ones to evaluate how the system evolves. This concept is widely used in nonlinear time series analysis for calculations in the attractor, see fig. 1. We are here applying it in the transient phase, so we need to have several close trajectories, which, in principle, may be generated numerically by changing slightly the initial conditions from the beginning of the integration procedure or at each time step.

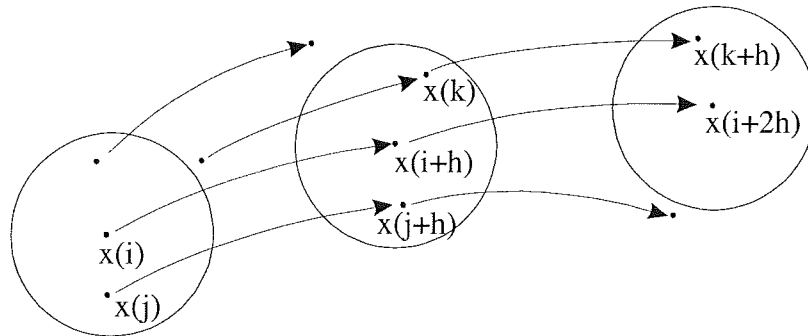


Figure 1. The balls of radius  $r$  centered at  $x(i)$ ,  $x(i+h)$  and  $x(i+2h)$  (Eckman and Ruelle, 1985).

However, if we can assume that the time step from one point to another in the time series is short enough that the Jacobian of the system has not substantially changed, then it should be possible to use only one trajectory by assuming that to pass from  $\delta\mathbf{x}(i)$  to  $\delta\mathbf{x}(i+h)$  we use  $\mathbf{J}$ , to pass from  $\delta\mathbf{x}(i)$  to  $\delta\mathbf{x}(i+2h)$  we use  $\mathbf{J}^2$ , to pass from  $\delta\mathbf{x}(i)$  to  $\delta\mathbf{x}(i+3h)$  we use  $\mathbf{J}^3$ , etc.

In this work we have tested several ways of calculating the divergence -using several trajectories and one trajectory- these are:

### 3.1. Volume (Area) Calculation

Assuming we have a set of nearby trajectories in phase space and using Eq. (16), it is possible to write:

$$V(t+h) = V(t) \cdot \exp \left[ \int_t^{t+h} \text{div}[J(x)] d\tau \right] \quad (17)$$

expanding the exponential function in Taylor series, we obtain:

$$V(t+h) = V(t) \left[ 1 + \int_t^{t+h} \text{div}[J(x)] d\tau \right] \quad (18)$$

the integral term may be expressed, using the trapezium rule, as:

$$\int_t^{t+h} \text{div}[J(x)] d\tau = \frac{(\text{div}[J_{t+h}] + \text{div}[J_t])h}{2} \quad (19)$$

Inserting Eq. (19) into Eq. (18) and regrouping the terms we obtain:

$$\frac{(\text{div}[J_{t+h}] + \text{div}[J_t])}{2} = \frac{1}{h} \frac{V(t+h) - V(t)}{V(t)} \quad (20)$$

Hence, when  $h \rightarrow 0$

$$\text{div}[J(x)] = \frac{\dot{V}(t)}{V(t)} \quad (21)$$

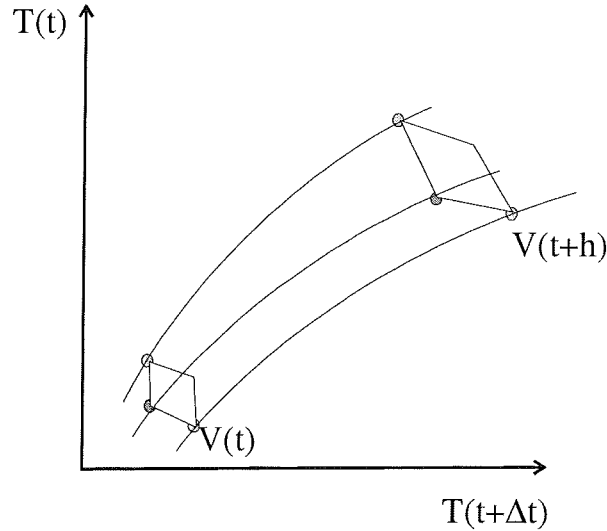


Figure 2. Representation of the evolution of the area (volume) for a reconstructed space in two dimensions using the reactor temperature.

This equation may be written in two different forms when using discrete time steps:

$$\text{div}[J(x)] = \frac{1}{h} \log \left( \frac{V(t+h)}{V(t)} \right) \quad (22)$$

or

$$\text{div}[J(x)] = \frac{1}{h} \left( \frac{V(t+h)}{V(t)} - 1 \right) \quad (23)$$

where  $V(t)$  is the area between three different points, see Fig. 2, or the volume in case of higher embedding dimensions ( $d_E > 2$ ), of the reconstructed space; and  $h$  is an appropriate time step.

### 3.2. Jacobian Reconstruction

Another way to calculate the divergence from numerical/experimental time series is to reconstruct directly the Jacobian and to calculate its trace. The time evolution of infinitesimal differences is completely described by the time evolution in tangent space, i.e. by the linearised dynamics. Let  $\mathbf{x}^{(1)}$  and  $\mathbf{x}^{(2)}$  be two such nearby trajectories in  $m$ -dimensional state space. Considering the dynamical system as a map, the time evolution of their distance is

$$\mathbf{x}_{n+1}^{(1)} - \mathbf{x}_{n+1}^{(2)} = \mathbf{F}(\mathbf{x}_n^{(1)}) - \mathbf{F}(\mathbf{x}_n^{(2)}) = \mathbf{J}_n (\mathbf{x}_n^{(1)} - \mathbf{x}_n^{(2)}) + O(\|\mathbf{x}_n^{(1)} - \mathbf{x}_n^{(2)}\|^2) \quad (24)$$

where we have expanded  $\mathbf{F}(\mathbf{x}_n^{(1)})$  around  $\mathbf{x}_n^{(2)}$  and  $\mathbf{J}_n = \mathbf{J}(\mathbf{x}_n^{(2)})$  is the  $m \times m$  Jacobian matrix of  $\mathbf{F}$  at  $\mathbf{x}^{(1)}$ .

For the case of a discrete system –experimental data points- it is possible to transform the linear equation, which represents the Jacobian evolution:  $\dot{\mathbf{y}} = \mathbf{J} \cdot \mathbf{y}$  into  $\mathbf{y}(t + \Delta t) = (\Delta t \cdot \mathbf{J} + \mathbf{I}) \cdot \mathbf{y}(t)$  - see Appendix 1- and then to calculate  $\mathbf{J}$  as a function of neighbour trajectories at each time step, whereas  $\mathbf{y} = \delta \mathbf{x}$ .

In order to calculate the Jacobian matrix, we need to solve a linear system equations given by the best linear fit of the map which for  $\mathbf{x}_n^{(1)}$  close to  $\mathbf{x}_n^{(2)}$  sends  $\mathbf{x}_n^{(1)} - \mathbf{x}_n^{(2)}$  to  $\mathbf{x}_{n+1}^{(1)} - \mathbf{x}_{n+1}^{(2)}$ . Close here means that the map should be approximately linear. Depending on the number of close trajectories,  $p$ , and the dimension of the system,  $m$ , we may have several situations. In the case of  $p < m+1$  the system is undetermined, if  $p = m+1$  it is possible to find an exact solution, and when  $p > m+1$  the system is overdetermined and we may find a least squares solution.

## 4. RUNAWAY DETECTION USING SIMULATED DATA

In order to avoid problems related to noise in the temperature measurements, we decided, as a first step, to use the simulated temperature data obtained from Zaldívar *et al.* (2002) for isoperibolic (constant jacket temperature) batch reactor in which different types of reaction take place (parallel, consecutive, etc.)

### 4.1. Preliminary analysis using all state variables

First, let us assume that we know all the state variables of the system, i.e. temperature and conversions. Then lets try to calculate the divergence of the system using these simulated data and

changing the different embedding parameters. This will give us a preliminary idea of the type of results we can expect in the best situation and will help us in studying which is the best numerical approach to follow.

- Divergence calculation with volume normalisation at each time step

In this case we have integrated the system (anchor trajectory) and in parallel, at each time step we have integrated a perturbed system consisting in several trajectories, each with one perturbed state variable, i.e.  $x_i = x_i^a \pm \delta$ . Hence, at each time step we force the value of  $V(t)$  and after integration we can obtain  $V(t+h)$  and calculate the divergence by applying Eq. (22) and/or Eq. (23). For example, Fig. 3 shows the divergence calculation using this approach for the case of a consecutive reaction carried out in an isoperibolic reactor in runaway conditions. Similar results are obtained by calculating the Jacobian, Eq. (24), using three trajectories. If we increase the number of trajectories and solve the overdetermined system by least squares the divergence calculation is improved (results not shown).

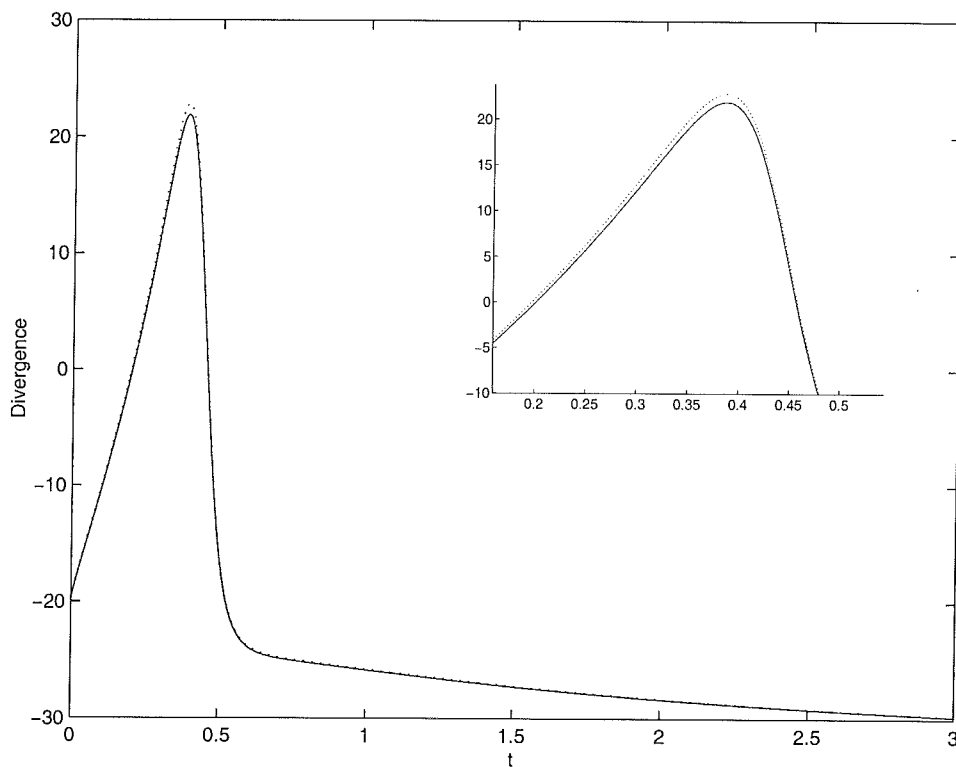


Figure 3. Calculated analytically (continuous) and numerically (discontinuous) –using the volume calculation technique with four trajectories,  $V(t)=10^{-9}$  - divergences for a consecutive runaway reaction carried out in an isoperibolic reactor (Zaldívar *et al.*, 2002). The region of maximum divergence has been amplified.

### - Divergence calculation without volume normalisation

This is the method we used in Strozzi *et al.* (1999) for an isoperibolic reactor in which a first-order reaction takes place. In this case, the trajectories are generated by changing slightly the initial conditions, instead that at each time step, i.e.  $x_i^0 = x_i^a \pm \delta$ . Figure 4a shows the results using the volume calculation technique for the non-runaway case of a consecutive reaction carried out in isoperibolic conditions, whereas in Fig. 4b the results obtained using the Jacobian reconstruction for the divergence with five trajectories are shown. As can be seen in both cases the calculation breaks down after a certain period of time. The same behaviour has been observed for other type of reactions, i.e. parallel, autocatalytic, first order (in this case is considerably less pronounced), etc. In order to study which are the reasons for this problem, we repeated the calculations but starting with the same initial conditions further in time, i.e. before the calculations do not work anymore. In these cases the calculations hold correct during a certain period of time and then they also break down. If we look at the areas calculated with the algorithm it is easy to understand the numerical instability that exists in this calculation, which is due to the general characteristic of dissipative systems, i.e. exponential volume contraction in state space. This can be observed in fig. 4c where in a logarithmic scale the numerically calculated  $V(t)$  versus the one obtained from the analytical divergence are depicted. As can be seen the analytical volume and the calculate coincide for a certain period until the  $V(t)$  is around  $10^{-19}$ , at this point the calculation is not valid anymore. This is due to finite numerical precision in the integration of the trajectories and to the fact that being a dissipative system the exponential volume contraction will, with sufficient time, require a computer precision not attainable. Hence, it is not possible, due to the exponential volume contraction in the state space to calculate the divergence of the system for all the simulation time using close initial conditions. This is due to the fact that the required numerical precision would, sooner or later, exceed the maximum computer precision and hence the calculation will break down. Of course, this is a numerical problem, which has no equivalence in a real reactor in which we are measuring temperatures. In this case, we are closer to the situation in which at each time step we are initialising the calculation procedure.

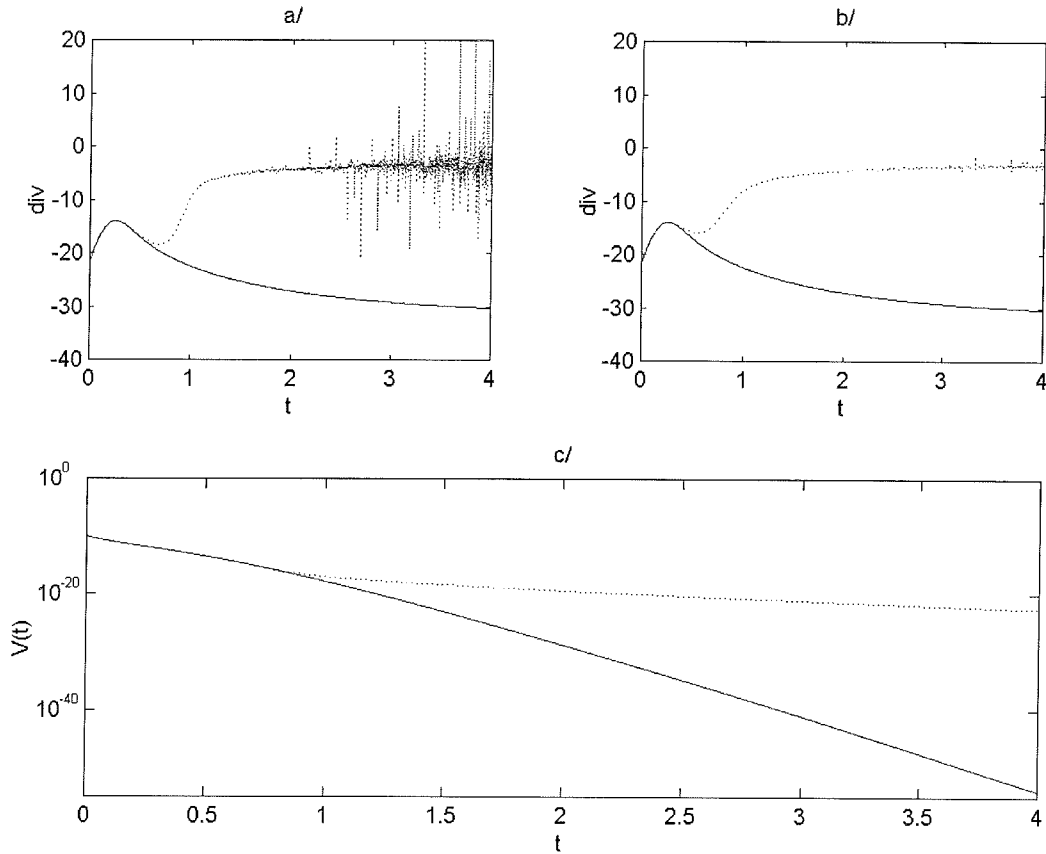


Figure 4. a/Calculated analytically (continuous) and numerically (discontinuous) divergences – using the Volume calculation technique with four trajectories- and b/calculated analytically (continuous) and numerically (discontinuous) –using the Jacobian calculation technique with six trajectories- for a consecutive non-runaway reaction carried out in an isoperibolic reactor (Zaldívar *et al.*, 2002) (See text for comments).c/  $V(t)$  calculated analytically (from the divergence) and numerically (discontinuous).

As we are interested only in the application of the runaway criterion, i.e.  $div > 0$ , and not in the exact calculation of the divergence, from Eq. (23) it is possible to see that the condition  $div > 0$  is equivalent to consider:

$$\frac{\Delta V(t)}{V(t)} > 0 \quad (25)$$

Due to the volume contraction in state space, characteristic of dissipative systems,  $V(t)$  will rapidly tend to zero and produce artefacts when introduced dividing in Eq. (25). However, by definition the volume is always positive and hence,  $div > 0$  is equivalent to check:

$$\Delta V(t) > 0 \quad (26)$$

This eliminates the need to calculate the division of two small numbers that produces an increase in the numerical errors of the calculation. Figure 5 illustrates this point for the case of runaway and

non-runaway in consecutive and parallel reactions. As can be seen analytical and calculated state space volumes are practically identical (the errors are one order of magnitude in relation to the absolute values), even though the numerically calculated divergence will not be correct after a certain amount of time, see fig. 4. Hence, from the point of view of numerical precision, it seems that instead of calculating the divergence is more advisable to compute the variation of volume in the state space. However, this has to be checked before using the reconstructed state space and the experimental data. Furthermore, as can be seen in fig. 5, for the case of a runaway, fig. 5a and 5c  $\Delta V(t) > 0$  whereas for the situation of nonrunaway, fig. 5b and 5d,  $\Delta V(t)$  never becomes positive, approaching zero.

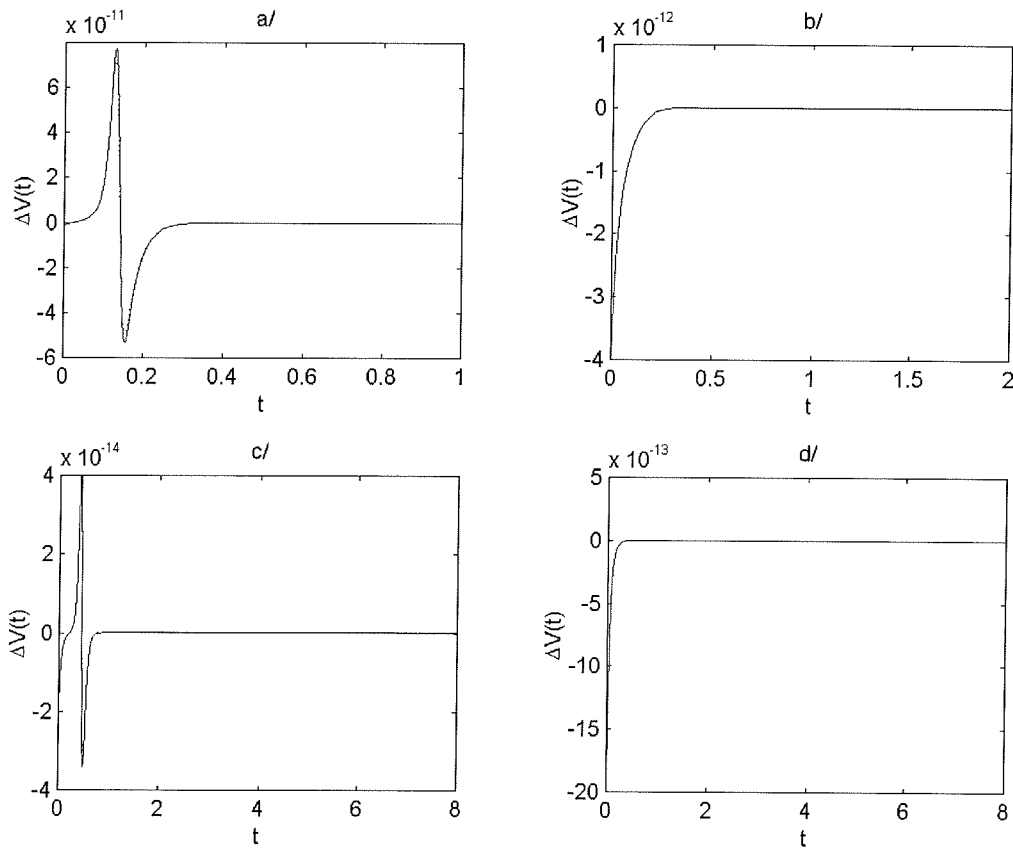


Figure 5. Analytical (continuous) and numerically (discontinuous) calculated state space volume variation,  $\Delta V(t)$ , for parallel and consecutive reactions in runaway and nonrunaway conditions. a/ Parallel-runaway; b/Parallel-nonrunaway; c/Consecutive-runaway; d/Consecutive-nonrunaway. For the runaway boundaries and operating conditions see Zaldívar *et al.* (2002).

#### 4.2. Physical interpretation of the numerical divergence criterion as a function of the embedding dimension

As by definition a volume (or area) cannot be negative, i.e.  $V(t) > 0$ , from Eq. (25) it is possible to see that the condition of  $div > 0$  is equivalent to consider  $V(t) > 0$  and  $\Delta V(t) > 0$ . If now we assume a

one-dimensional system (in this case we are dealing with lengths, not areas or volumes) we can easily see that  $V(t) = \Delta T(t)$  and that  $\Delta V(t) = \Delta^2 T(t)$ . This is equivalent to Hub and Jones (1986) criteria, which used the increase of the heat evolution as the hazard identification criterion, i.e:

$$\frac{dq_G}{dt} > 0 \quad (27)$$

where  $q_G$  is the power generated by chemical reaction. The principle applied is based on a simple energy balance over the reactor:

$$q_G = MCp \frac{dT}{dt} + US(T - T_e) \quad (28)$$

Power generated = power used to increase the temperature of the reaction mixture + power removed by the coolant flowing through the jacket. From expression Eq. (28) it is possible to obtain:

$$\frac{dq_G}{dt} = MCp \frac{d^2T}{dt^2} + US \frac{d(T - T_e)}{dt} \quad (29)$$

assuming that  $MCp$  and  $US$  are constants over time.

The criterion of Eq. (27) defines two different regions separated by the line  $dq_G/dt = 0$ . The region in which the heat output of the reaction declines can be considered non-hazardous. However, two other zones in the region in which the heat output of the reaction increases, can be discarded from the potentially dangerous region. In the former, the power accumulated in the reaction mixture increases and the power removed through the jacket decreases; this is due to deliberate heating of the heat transfer fluid by the control system and, in principle, is not dangerous. In the latter, the heat removed increases and the heat accumulated decreases, so in this situation the reaction is under control. Hence, for the purpose of hazard recognition it is sufficient to check the following two expressions:

$$\frac{d^2T}{dt^2} > 0 \text{ and } \frac{d(T - T_e)}{dt} > 0 \quad (30)$$

which for the case of isoperibolic reactors, i.e. constant jacket temperature, simplifies to consider  $dT/dt > 0$ . By comparison, it is possible to see that Eq. (25) is the discrete version of Eq. (30) since we have requested  $\Delta T(t) > 0$  and  $\Delta^2 T(t) > 0$ . Hence assuming only one embedding dimension we can obtain the Hub and Jones (1986) criterion. Even though this criterion is independent from the characteristics of the process we are supervising, i.e. we need only to measure the temperature and calculate its derivatives, the method has the problem of noise amplification. Furthermore, as it was shown by Strozzi *et al.* (1999) the criterion does not work for certain types of reactions as for example autocatalytic reactions. From the dynamical systems point of view, this can be seen as the

fact that using only one dimension we are not able to unfold the underlying dynamics of our system and hence as we do not have an embedding we are not able to calculate correctly its divergence.

Lets see what happens when we increase the embedding dimension to two. In this case, the application of the criterion  $div>0$  gives the following equations:

$$V = \Delta T \cdot \Delta z \quad (31)$$

$$\Delta V = \Delta(\Delta T \cdot \Delta z) \quad (32)$$

As  $V>0$  by definition, it follows that for having  $div>0$  then  $\Delta V>0$ , which can be expressed as:

$$\frac{\Delta^2 z}{\Delta z} + \frac{\Delta^2 T}{\Delta T} > 0 \quad (33)$$

which, in continuous terms may be written as:

$$\frac{d^2 z/dt^2}{dz/dt} + \frac{d^2 T/dt^2}{dT/dt} > 0 \quad (34)$$

Hence, if we have said before that for being in runaway conditions we need to have both the first and second derivatives of reactor temperature positive, then in two dimensions we found the next condition for runaway: the ratio between acceleration and velocity conversion should not be lower than minus the ratio between temperature acceleration and temperature velocity. This is a further restriction that takes into account the role of conversion and makes it possible to distinguish between runaway and nonrunaway in autocatalytic reactions, eliminating the problem of false alarms due to the runaway criterion employed.

Based on this physical interpretation, we can now discuss the role of the embedding dimension in the divergence reconstruction. As said before, if we assume that our system may be reconstructed in one dimension we will obtain the Hub and Jones criterion (1986). However, this criterion is not valid for certain types of reactions (Strozzi *et al.*, 1999), hence, it is necessary to work at least in dimension two.

### 4.3. Reconstruction using time delay vectors, derivatives and integrals

In this work, we have assessed several reconstruction techniques, i.e. time delayed vectors, derivatives and integrals. Even though, theoretically, all the methods of reconstruction should produce the same result, there is no a priori method to decide which is the more adequate (Casdagli *et al.*, 1991) and there is a considerable difference in the quality of the resulting reconstructed state space coordinates and hence in the calculated quantities from these coordinates. The lack of a unique solution for all purposes is due in part to the presence of noise and the finite length of the

data set (Breedeen and Packard, 1994). Furthermore, in our case the situation is complicated by the nonstationarity of our system.

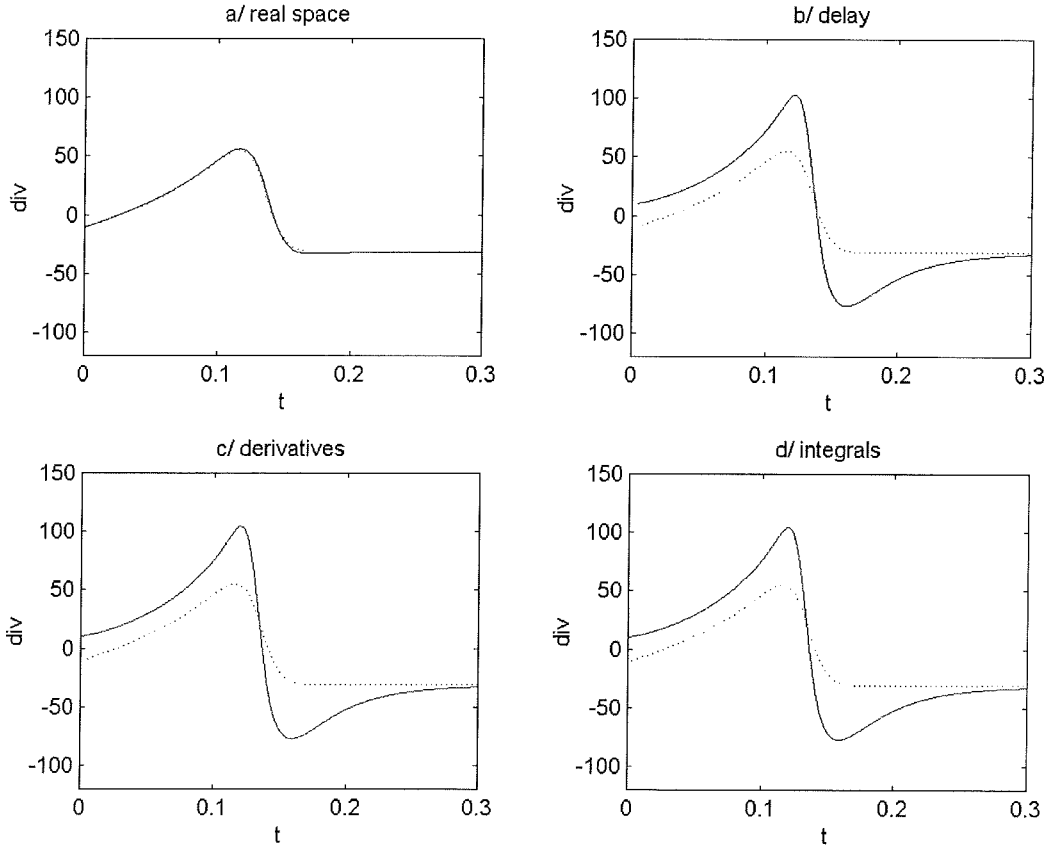


Figure 6. Analytical (discontinuous) and reconstructed (continuous) divergences calculated using Eq. (23) with  $d_E = 2$  for the case of a parallel-runaway reaction. a/ Real state space  $\{T(t), x(t)\}$ ; b/ delayed time vectors  $\{T(t), T(t-\Delta t)\}$ ,  $\Delta t=0.005$ ; c/derivatives  $\{T(t), dT(t)/dt\}$ ; d/ integrals  $\{T(t), I_1[T(t)]\}$ .

We have tested the reconstruction in the three state spaces, delayed vectors, derivatives and integrals. As can be seen in Fig. 6 for the case of a parallel-runaway reaction all the three state spaces produce very similar results. This is true also in all the cases studied and, hence, we may conclude that, in absence of noise, all the three techniques to calculate the divergence of our system produce similar results. Therefore, in order to select the most appropriate reconstruction technique we have to analyse the results from experimental data when noise and fluctuations will appear. Furthermore, as can be seen, an embedding dimension of two is enough to reconstruct the divergence of our systems.

In order to select the appropriate parameters we have run several tests by changing the number of temperature measurements (trajectories) and the embedding dimension using the reconstruction based on derivatives. Figure 7 shows the calculated  $\Delta V(t)$  as a function of the number of

temperature trajectories and embedding dimension. As can be seen, in all the cases  $\Delta V(t)$  becomes greater than zero and hence we are able to detect the runaway. However, the better results in terms of curve similarity are obtained with one temperature trajectory and  $d_E = 2$ , fig. 7b, and three temperature trajectories and  $d_E = 2$ , fig. 7c. Increasing one dimension,  $d_E = 3$ , does not improve the results, even though the system has three state variables. This is due to the fact that as all dissipative system the isoperibolic batch reactor is decreasing its dimension to zero (fixed point at the end of the reaction), and hence an embedding dimension of two seems to represent better the system during all its dynamics. Another point to notice is that the values obtained of  $\Delta V(t)$  using different reconstruction schemes are different, even though the divergence is similar. This is due to the fact that the divergence is a preserved quantity under state space reconstruction (Strozzi, 1997) which is not the case for  $\Delta V(t)$ .

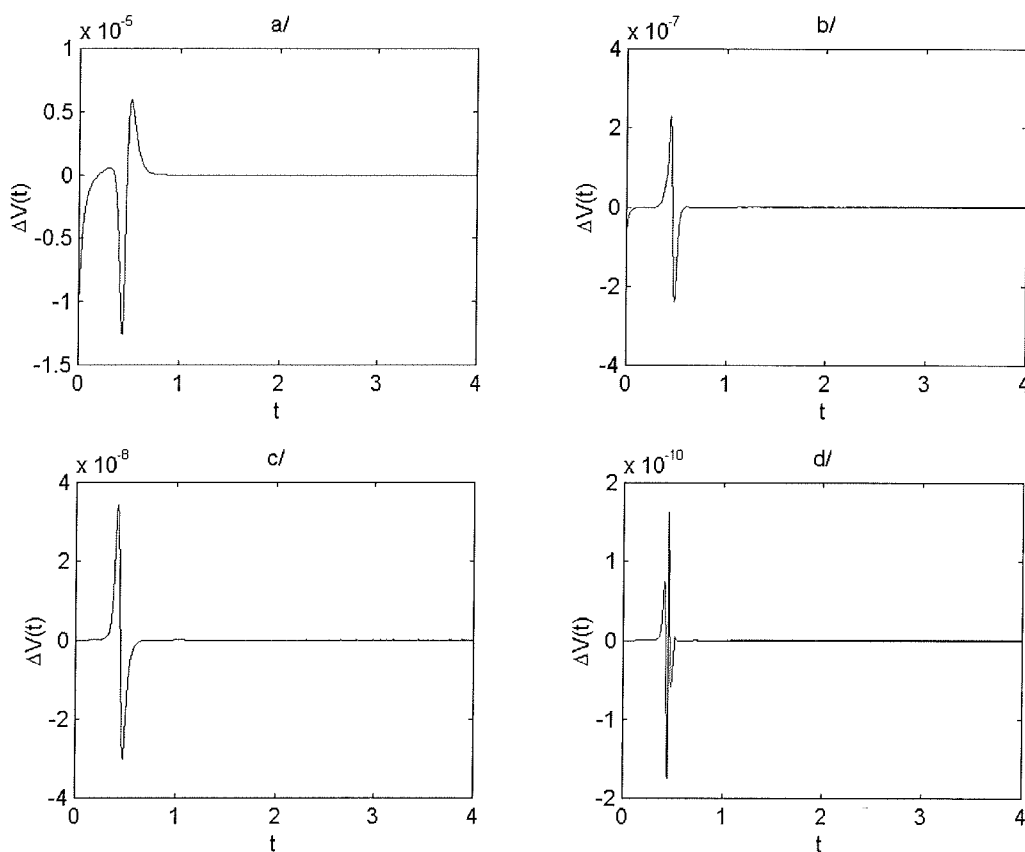


Figure 7. Reconstructed  $\Delta V(t)$  for the case of a consecutive-runaway reaction using: a/ One temperature trajectory,  $d_E = 1$ ; b/One temperature trajectory,  $d_E = 2$ ; c/Three temperature trajectories;  $d_E = 2$ ; d/ Four temperature trajectories;  $d_E = 3$ .

Similar results are obtained for the case of consecutive-nonrunaway, see Fig.8. However, in this case, even though the curves are similar, only the reconstruction using three temperature trajectories

and  $d_E = 2$  will not produce a false alarm, Fig. 8c, since in all the other cases  $\Delta V(t)$  crosses the zero. Of course in case of noise superimposed to the signal one has to establish an upper limit and hence this problem can be corrected.

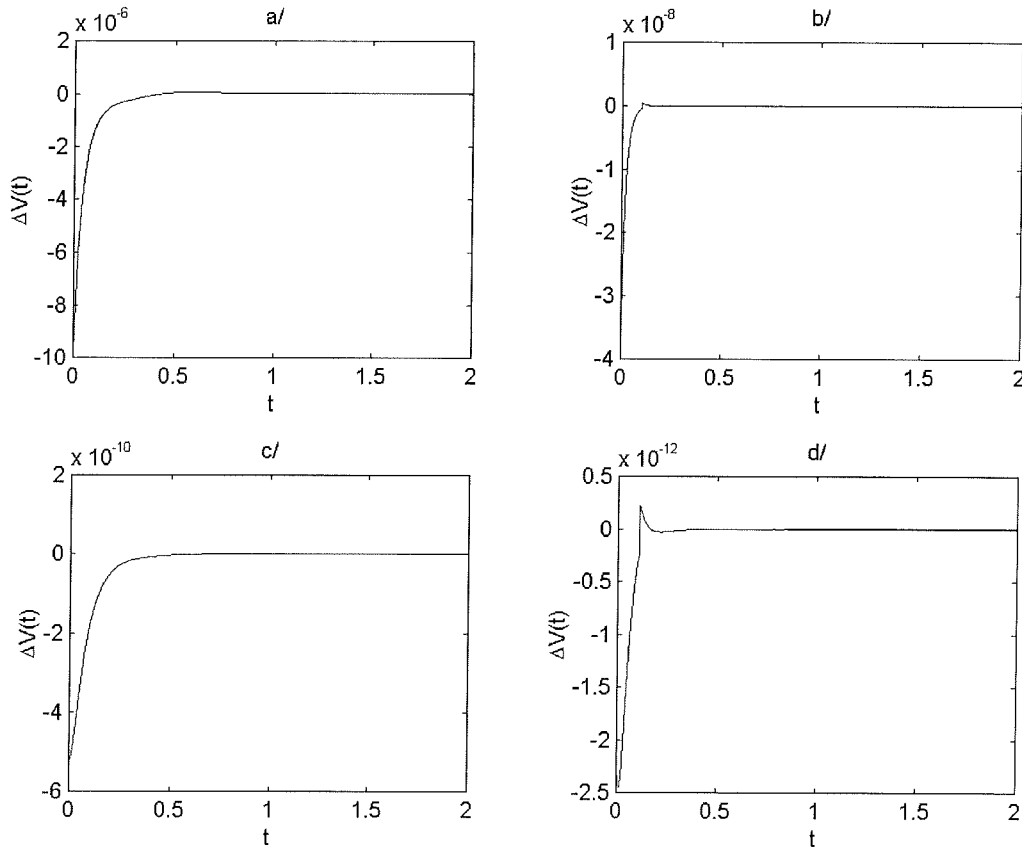


Figure 8. Reconstructed  $\Delta V(t)$  for the case of a consecutive-nonrunaway reaction using: a/ One temperature trajectory,  $d_E = 1$ ; b/One temperature trajectory,  $d_E = 2$ ; c/Three temperature trajectories;  $d_E = 2$ ; d/ Four temperature trajectories;  $d_E = 3$ .

As conclusions of this theoretical study, in absence of noise it is not possible to establish which is the best reconstruction space, i.e. time delayed vectors, integrals or derivatives, since all produce similar results. The addition of a certain amount of white noise has not been considered, since it is not the only noise existing in the real system and hence the results would not be meaningful, see next Section. Concerning the embedding dimension, it seems that a value of two is the most appropriate, using three temperature trajectories. Of course, from the practical point of view, it would be more appropriate to use only one temperature measurement than having three sensors inside the reactor.

## 5. RUNAWAY DETECTION USING EXPERIMENTAL DATA

State space reconstruction techniques and divergence calculation have been applied to several experimental data sets in order to test the different algorithms for early warning detection of runaway initiation based on the divergence criterion.

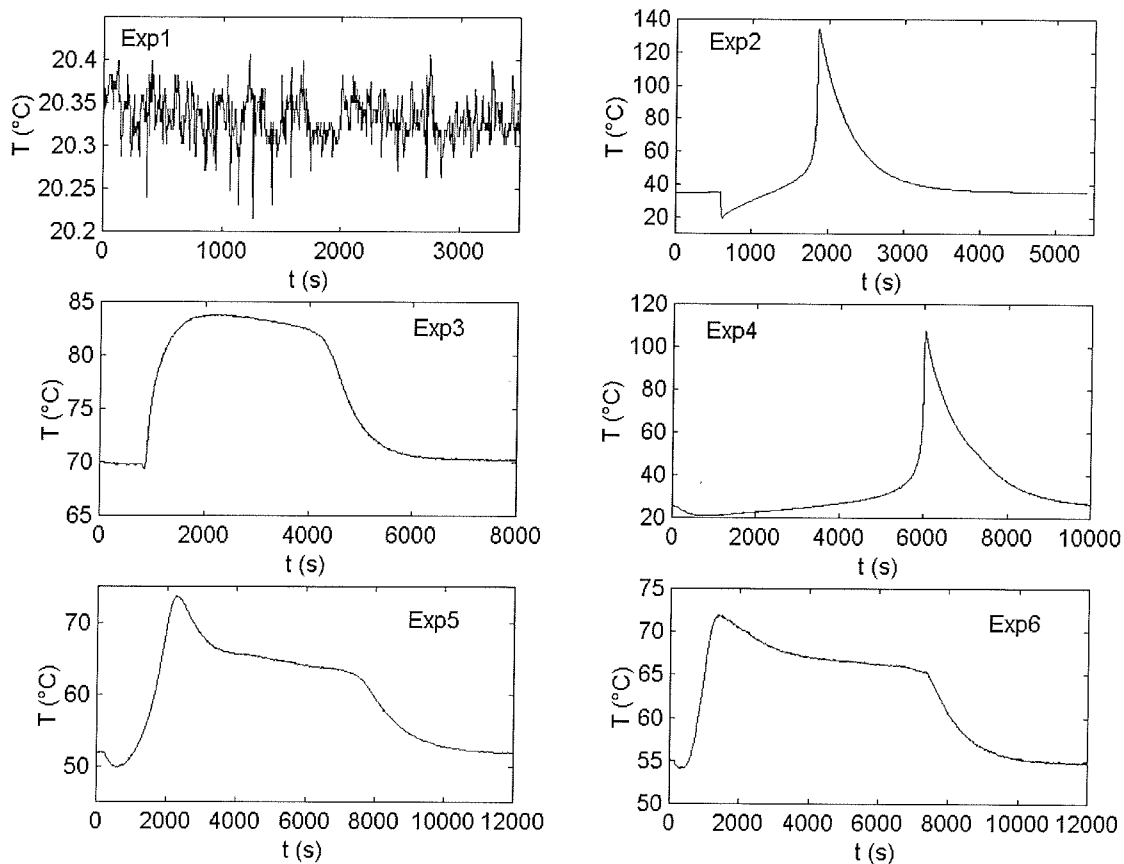


Figure 9. Experimental Reactor temperature profiles for the bench scale (2L) batch and semibatch reactor experiments (Exp1, Exp2 and Exp3) and for the 100 L pilot plant semibatch reactor experiments (Alós *et al.*, 1998): Exp4, Exp5 and Exp6.

### 5.1. Description of the experimental data sets

The data sets are part of several experimental campaigns carried out in different reactors, i.e. a 2 L bench-scale reactor (Zaldívar *et al.*, 1996) and 100 L Pilot plant reactor (Zaldívar *et al.*, 1993). The chosen reaction was the esterification reaction between 2-butanol and propionic anhydride catalyzed by sulphuric acid that has been extensively studied (Snee *et al.*, 1992; Galván *et al.*, 1996).

#### - Bench-scale experiments (2L)

In these experiments, twelve temperature sensors (thermocouples), six in each probe, were placed inside the 2L bench-scale reactor. The temperature profiles for several of these experiments are

summarised in Figure 9. Exp1 represents a calibration experiment with the reactor filled with water, constant jacket temperature and 400 rpm of stirrer speed. Exp2 shows a typical runaway profile obtained with the esterification reaction. The experiment was carried out in batch isoperibolic conditions,  $T_{jacket} = 35$  °C. Exp3 is also an esterification reaction in isoperibolic conditions,  $T_{jacket} = 70$ °C, stirrer speed 400 rpm, but instead of a batch process, we carried out the reaction in semibatch conditions with 1 hour of feeding (dosing) time at constant rate. These conditions were selected to have a quasi-instantaneous reaction rate, QFS temperature profile (Quick onset, Fair conversion and smooth temperature profile) (Steensma and Westerterp, 1990), which, in principle, should not give an alarm, even though that we are on ignition conditions that is normally the optimum strategy to carry out semibatch processes (Alós *et al.*, 1998).

- *FIRES (Facility for Investigating Runaway Events Safely) experiments (100L)* (Zaldívar *et al.*, 1993)

Three isoperibolic semibatch experiments were carried out in the pilot plant facility using also the esterification reaction between 2-butanol and propionic anhydride. The temperature inside the reactor was measured using 3 Pt100 sensors in a probe. The reactor was charged with 405 mol of 2-butanol with the appropriate amount of sulphuric acid. When the reactor temperature was stabilised at the jacket temperature, 405 mol of propionic anhydride were added at constant rate for 2 hours. The experimental temperature profiles have been plotted in Fig. 9. As can be seen, Exp4 shows a typical runaway profile whereas Exp5 approximate to a QFS profile (Quick onset, Fair conversion and smooth temperature profile) (Steensma and Westerterp, 1990), even though there is an initial temperature jump. Exp6 is closer to a QFS than Exp5. An example of typical QFS profile using the same reacting system can be seen in Exp3 in the bench-scale reactor experiments.

## 5.2. Nonlinear noise reduction

Any measurement, in this case temperature, contains a part of interest, the signal, and a part that does not contain any information about the variable we are studying, the noise. Generally, this type of noise is called additive, measurement noise, or observational noise i.e.

$$s(t) = y(t) + \sigma(t) \tag{35}$$

Observational noise does not affect the evolution of the dynamical system. In such a case one can hope to identify it and to be able to subtract it from the recorded data in order to find the unperturbed signal. This case is different from the case of dynamical noise where the noise acts directly on the state of the dynamical system influencing its evolution, for example:

$$\frac{d\mathbf{x}}{dt} = \mathbf{F}(\mathbf{x}, \alpha) + \sigma(t) \quad (36)$$

In this case the noise is embedded in the system and sometimes acts as a driving function of the system. For dynamical noise, the techniques we are going to discuss here are not valid. However, it is difficult to distinguish between observational and dynamical noise since they may not be distinguishable *a posteriori* based on the data available. For example, when measuring temperatures in a stirred chemical reactor we may have some additive noise from the measurement itself but another part maybe due to the fact that our system is a three dimensional inhomogeneous turbulent system and, hence, temperature fluctuations are real and not the result of noise introduced by the measurement system.

As it has been commonly observed, the effects of relatively small amount of observational noise may put severe restrictions on the characterisation and estimation of the properties of the underlying dynamical system. In order to remove the observational noise, different possibilities are available which can be broadly divided into two categories: linear filters which are based on the application of Fourier techniques, and non-linear noise reduction methods that make use of the deterministic origin of the signal we are interested in.

Linear digital filters have been developed to eliminate noise at high, low or specific frequencies (notch filters, for example to take out the 50 Hz AC contamination in signals recorded with electronic circuits), respectively, and there is a vast amount of literature and algorithms developed for such a purpose (Oppenheim and Schaffer, 1975; Goodwin and Sin, 1984; Press *et al.*, 1986; Treichler *et al.*, 1987; Haykin, 1991; amongst others). In the statistical approach to the solution of the linear filtering problem an useful approach is to minimise the mean square value of the error signal that is defined as the difference between some desired response and the actual filter output. For stationary inputs, the resulting solution is commonly known as the Wiener filter, which is said to be optimum in the mean square sense.

If the nonlinearity tests are positive and hence, one may assume that the data originated from a deterministic nonlinear system, then methods for nonlinear noise reduction may be applied. The basic idea of all these methods is to exploit the underlying determinism by correcting the states and the time series values using a model that is previously fitted to the raw data - for a recent survey see Kostelich and Schreiber (1993), and Davies (1994). The main objective as opposite to linear filtering techniques resides in the fact that one tries to maintain the general characteristic that dissipative motion tend to occupy smooth submanifolds of the total available state space. These methods share the following common similarities (Kostelich and Schreiber, 1993):

- a/ a strategy for reconstructing the underlying attractor;
- b/ a class of models with fitting parameters to estimate the local dynamical behaviour in the reconstructed system;
- c/ a method to adjust the observations to the selected model.

Both, linear and nonlinear filtering techniques assume we are dealing with a stationary signal and there is only observational noise. Since batch and semibatch reactors are non-stationary by definition we cannot exclude the existence of dynamical noise, but the situation is the same for a large number of real applications, and hence, caution should be taken when applying techniques that have been developed and tested for systems with fundamentally different characteristics. Furthermore, for the case of nonlinear filters there is a need for data redundancy, i.e. suitable neighbours in state space. If there are not enough or a particular region in the state space is empty nothing can be done to filter the signal. This is, as we will see later on, particularly important in our case where we are studying temperature trajectories. A particular temperature trajectory in the reconstructed state space will rarely return closely to itself, and, hence data redundancy is more difficult to assure. However, this may be obtained by using several measurements at different locations in the reactor. The interest is that nonlinear filters have proved to be superior to adaptive linear filters for example in human voice treatment, which is a non-stationary, not deterministic signal (Hegger *et al.*, 2000). Furthermore, nonlinear filters will preserve nontrivial high order statistics and, hence, the divergence of the system, in principle, should be better maintained using this type of techniques.

In this work we have applied the modified (Schreiber and Richter, 1999) nonlinear local projective noise reduction algorithm developed by Grassberger *et al.* (1993). This method assumes that the deterministic part of the time series,  $y(t)$ , Eq. (35), lies on a low-dimensional manifold,  $d_q$ , in a high-dimensional reconstructed state space,  $d_E$ , while the effect of the noise is to distribute the data randomly in the surroundings of the manifold. Interested readers are referred to Kantz and Schreiber (1998) and references therein for a detailed description of the method and relevant discussions. This noise reduction scheme has been implemented in the TISEAN software package (Hegger *et al.*, 1999) by the routine *ghkss*.

Until recently, all the nonlinear filtering methods proposed in the literature were formulated as *a posteriori* filters, i.e. batchwise using all the data set. Furthermore, the proposed filtering algorithms were quite computer time intensive. In order to overcome these two problems, Schreiber and Richter (1999) have recently modified their local projective noise reduction scheme (Grassberger *et*

*al.*, 1993) in such a way that its use in real time signal processing is feasible. The modifications can be summarised as follows (Schreiber and Richter, 1999):

- The local neighbours used are points in the past and, hence, no noise reduction occurs at the beginning.
- The number of local neighbours to carry out the correction has been limited.
- The dynamics is supposed to vary smoothly in state space, which practically means that the algorithm stores the linear approximation in state space only for a collection of representative points, reducing the number of times the local linear problem has to be solved.

The method has been developed and implemented in the TISEAN software package (Hegger *et al.*, 1999) by the routine *noise*, and it has been tested in different application with considerable improvements over traditional filtering (Hegger *et al.*, 2002).

- Application of nonlinear local projective noise reduction to reactor temperature data:

In order to apply the on-line projective noise reduction algorithm to reactor temperature data it is necessary to define a number of parameters, between them the embedding dimension,  $d_E$ , and the time delay,  $\Delta t$ , which are the reconstruction parameters, the dimension of the manifold to project onto,  $d_q$ , the minimal diameter,  $\varepsilon$ , the desired maximal number of neighbourhoods, and the maximal time in the past considered as neighbours,  $t_p$  (Hegger *et al.*, 1999). As said before, our system is a nonstationary system and, hence, the notion of a “correct” embedding or delay is inappropriate as has been demonstrated by Grassberger *et al.* (1991). Furthermore, we know that the attractor is a fixed point, when the reaction has finished and all the reagents have been depleted, hence, a fixed point has zero dimension. However, the initial dimension will depend on the type of reactive system we are dealing with, i.e. number of reactions that contribute to the heat of reaction and on the type of operating conditions we choose, for example in the case of isoperibolic conditions, only the reactor temperature has to be considered, whereas in the case of isothermal conditions the jacket (heating/cooling circuit) temperature has also to be taken into account (Zaldívar *et al.*, 2002). Hence the dimension of our non-stationary system is changing with time. As discussed before, a solution to this problem is by overembed the time series, so we have used embedding dimensions between 7 and 10 which seems adequate in function of our experience with Recurrence Quantification Analysis (RQA) where we used a dimension of 10 (Zbilut *et al.*, 2002). The same type of considerations applies when selecting the time delay. In this case several time delays going from 1 to 10 have been studied. As the real dimension of our system changes normally from for example three in isoperibolic batch parallel or consecutive reactions to zero, one should expect that

the dynamics confine the trajectories to a lower dimensional manifold  $d_q$  with dimensions between 1 and 3. Several tests have been done using different number of embedding dimensions to unfold and to project, several neighbours ratios, time in the past considered, etc. For a detailed discussion on the filter parameters selection the reader is referred to Bosch *et al.* (2002) where all the different tests are described.

Figure 10 shows the filter results during several instants of Exp6 in the 100 L pilot plant reactor. As can be seen, the filter is able to work properly in the presence of a considerable amount of noise, due to some problems with the insulation of the ground in the plant facility. Another characteristic of the filter is that no corrective action is taken when no neighbours are found, beginning of fig 10b. This in our case is an advantage over traditional FIR filters as moving average or Savitzky-Golay filters that will modify the dynamics of the system in case of a fast change, i.e. reactant addition, temperature stabilisation, etc. which are typical of batch and semibatch processes (Bosch *et al.*, 2002).

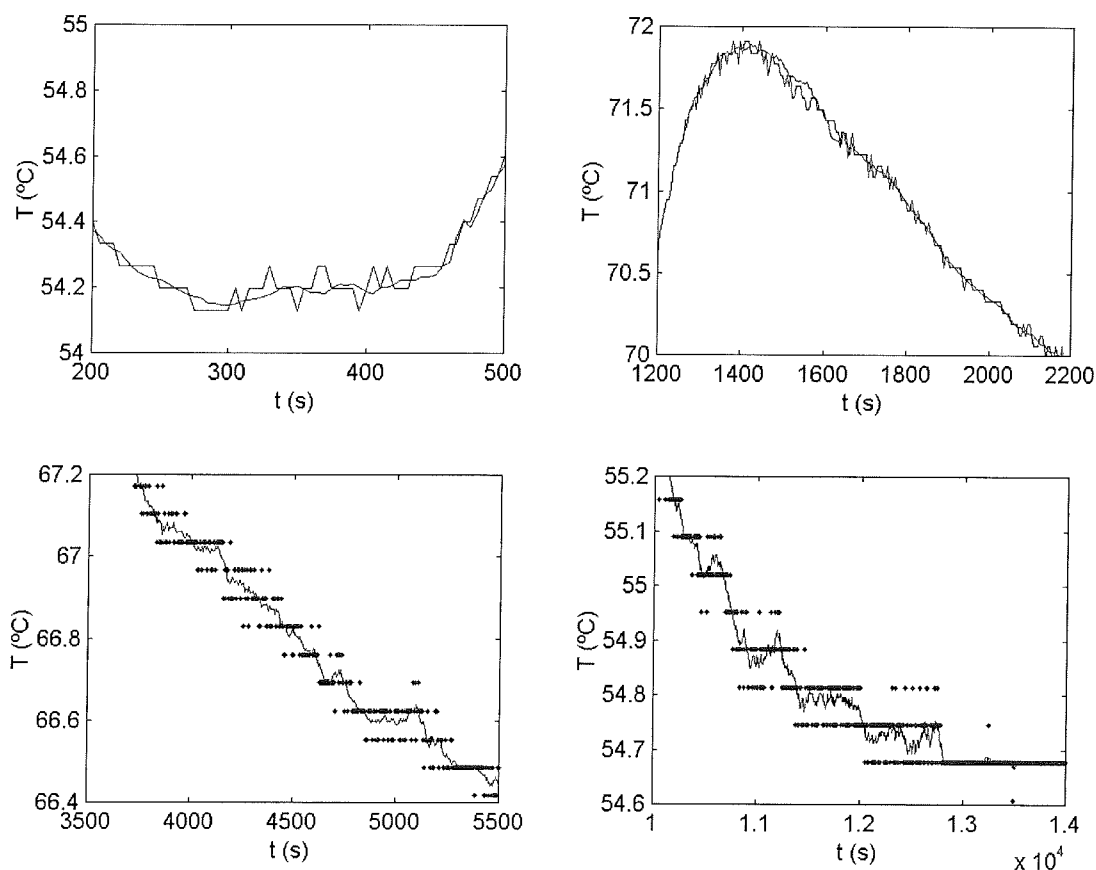


Figure 10. Experimental and filtered temperature data for the experiment Exp6 in the 100 L pilot plant reactor. Parameters:  $d_E=7$ ,  $d_q=2$ ,  $\Delta t=1$ ,  $\varepsilon=0.5$ ,  $t_p=300$ .

### 5.3. Runaway detection

In order to test which are the best method and parameters for calculating the divergence using experimental data, we have carried out several calculations using the derivatives state space reconstruction. Even though time delayed vectors is the most usual state space reconstruction method, for the case of nonstationary signals as the temperature in discontinuous reactors, it is not clear how to calculate an “optimum” time delay and hence derivatives are preferred. Furthermore, they have a clear physical meaning as has been discussed in Section 4. Finally, in the cases studied, the results obtained using state space reconstruction with integrals are similar to the ones obtained with derivatives.

Figures 11-13 show the results for the case of one and three filtered temperature trajectories. The nonlinear filter is able to remove a considerable amount of noise and to smooth the results. As can be seen, all methods distinguish between nonrunaway (Exp1) and runaway (Exp2 and Exp4). Exp 3 may be considered as a nonrunaway case, QFS, however, there is a temperature acceleration at the beginning of the reaction. Exp5 and Exp6 are closer to nonrunaway conditions, i.e. QFS but still there is an acceleration in the reactor temperature due to an accumulation of reagent at the beginning of the reaction (Alós *et al.*, 1997).

Figure 11 shows the results for the case of one filtered temperature trajectory. In this case we have used the Jacobian reconstruction procedure to calculate the divergence. The derivatives are calculated using a five points equation (Burden and Faires, 1996). In order to avoid the problem of division by a small number, see Section 4, there is a volume limitation into the algorithm, i.e. when  $V(t) < 0.0015$  the divergence is not calculated and its value assigned arbitrary to  $-0.1$ . As can be seen this is always the case in Exp1 and in long parts of the other experiments. However, it is possible to see that the runaway is detected. For the detection procedure, we have distinguished between, first type of alarm ( $\text{div} < 1.27$ ) and second type of alarm ( $> 1.27$ ). For the case of the 2 L reactor, there will be an alarm during the addition in Exp2 that can be easily separated from runaway as there is a decrease in temperature. In this case state space volume is increasing mainly due to inhomogeneities as consequence of the batch introduction of the second reagent. Furthermore, there will be a first type alarm at 1564 s and it will become second type alarm at 1832 s. The maximum reactor temperature is reached at 1872 s. Exp3 will give a first type alarm at 930 s and no alarm afterwards. For the 100 L experiment with one temperature trajectory Exp4 a first type alarm will be produced from 5758 s, whereas the second type alarm will occur at 5928 s. In this case, the reactor maximum temperature is reached at 6025 s. Exp5 and Exp6 will give a first type alarm at 1735 s, and 900 s respectively and no alarm afterwards.

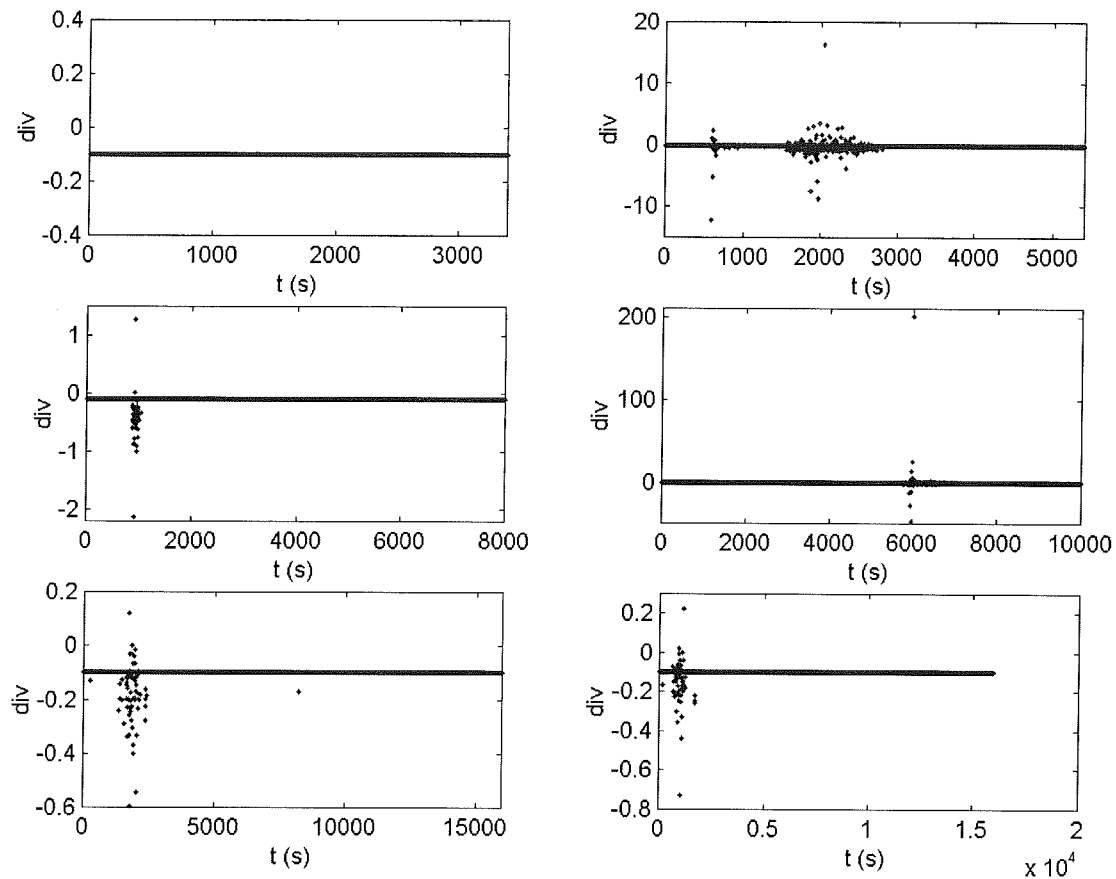


Figure 11. Reconstructed divergence using one filtered temperature trajectory and an embedding dimension of 2 for the experiments described in Figure 9.

For the detection procedure, for the case of the 2 L reactor, using one temperature trajectory, Fig. 12, we have distinguish between background noise ( $4 \cdot 10^{-3}$ ), first type of alarm ( $< 3 \cdot 10^{-2}$ ) and second type of alarm ( $> 1.1 \cdot 10^{-1}$ ). With this procedure, there will be an alarm during the addition in Exp2 that can be easily separated from runaway as there is a decrease in temperature. In this case state space volume is increasing mainly due to inhomogeneities as consequence of the batch introduction of the second reagent. Furthermore, there will be an alarm of the first type from 1700 s, whereas the alarm of the second type will start after 1750 s. The maximum reactor temperature is reached at 1872 s. Exp3 will give a first type alarm at the beginning, between 860 and 950 s an no alarm afterwards. For the 100 L experiment with one temperature trajectory Exp4 a first type alarm will be produced from 5830 s, and the second type alarm will occur at 5860 s, whereas the reactor maximum temperature is reached at 6025 s. Exp5 and Exp6 will give a fist type alarm at the beginning, between 1400-2100 s, and between 600 -1200 s, respectively and no alarm afterwards.

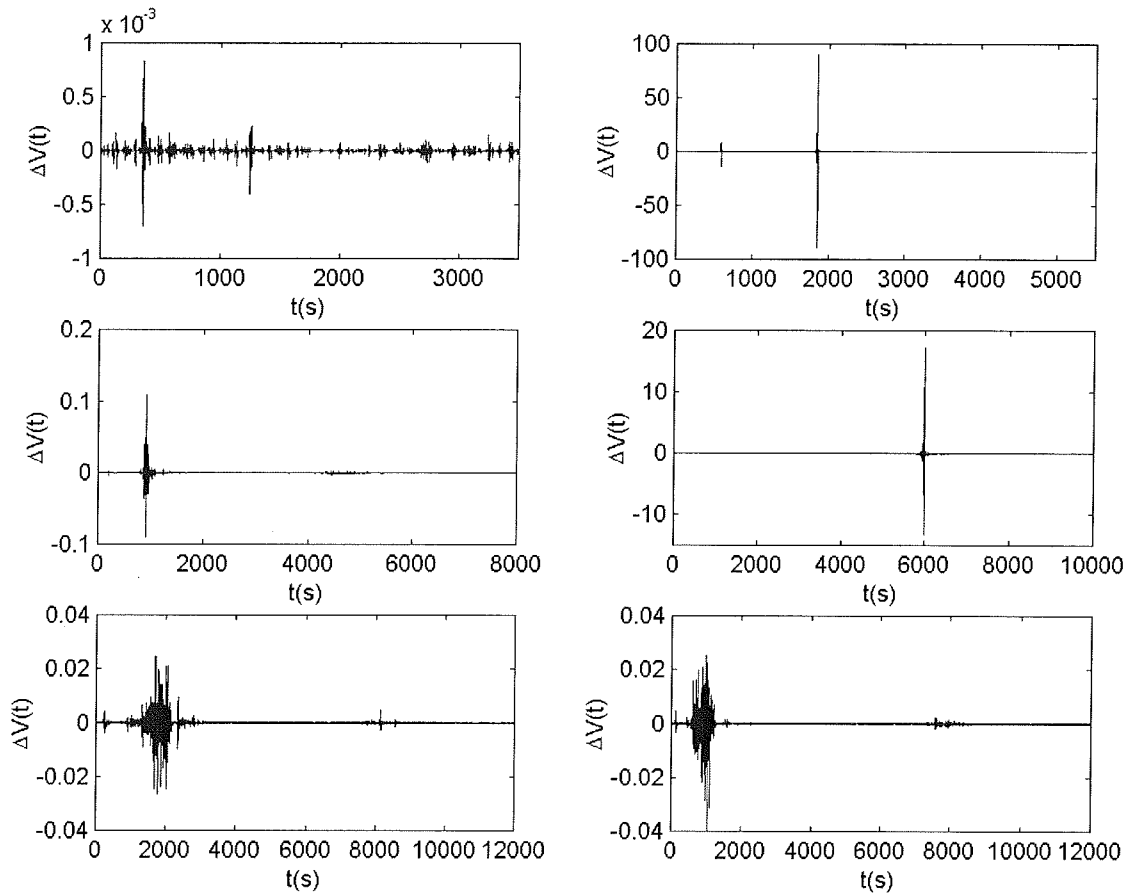


Figure 12. Reconstructed  $\Delta V(t)$  using one filtered temperature trajectory and an embedding dimension of 2 for the experiments described in Figure 9.

For the detection procedure, for the case of the 2 L reactor, using three temperature trajectories, Fig. 13, we have distinguish between background noise ( $2 \cdot 10^{-3}$ ), first type of alarm ( $< 4 \cdot 10^{-2}$ ) and second type of alarm ( $> 4 \cdot 10^{-2}$ ). With this procedure, there will be an alarm during the addition in Exp2 as in the previous case. Furthermore, there will be an alarm of the first type from 800 s, whereas the alarm of type 2 will start after 1830 s. The maximum reactor temperature is reached at 1872 s. Exp3 will give a first type alarm at the beginning, between 860 and 1050 s and no alarm afterwards. For the 100 L experiment with three temperature trajectories Exp4 several alarms of first type will be produced from 800 s onwards, continuous from 5696 s, and the second type alarm will occur at 5750 s, whereas the reactor maximum temperature is reached at 6025 s. Exp5 and Exp6 will give a first type alarm at the beginning, between 1500-2000 s, and between 600 -1100 s, respectively and no alarm afterwards.

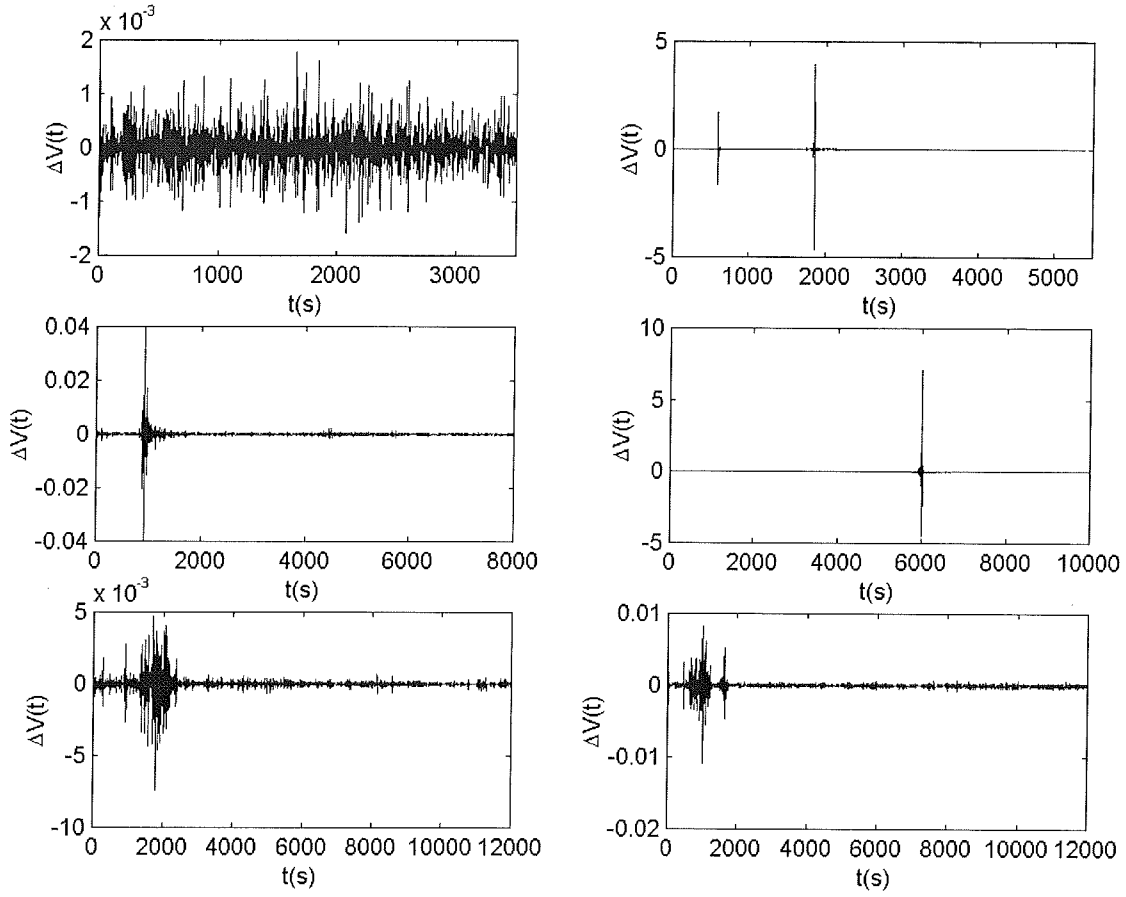


Figure 13. Reconstructed  $\Delta V(t)$  using three filtered temperature trajectories and an embedding dimension of 2 for the experiments described in Figure 9.

As can be seen from the results all the procedures give similar results. In the case of the calculation of the divergence using the Jacobian, the detection occurs later than using  $\Delta V(t)$ . This is mainly due to the fact that the imposed minimum volume restriction does not allow the calculation of the divergence for long periods of time. A lower volume limit will allow its calculation but will amplify the errors. The use of only one temperature trajectory gives earlier detection for the 2 L reactor but later for the case of the 100 L reactor. Even though, using simulated data the option of three temperature trajectories produced more correct results, in the case of experimental data this is not true anymore. In this case noise and real fluctuations and inhomogeneities in the reactor play an important role.

Finally, even though the divergence should be preserved under state space reconstruction, but the state space volume variation no. We have to check that  $\Delta V(t) > 0$  as our alarm criterion. However, it is clear that with experimental data some limits have to be established and that these limits would

depend on the type of reactor and the temperature measurement device installed and, in consequence, calibration will be necessary, but this is can be easily automated.

## 6. CONCLUSIONS AND FUTURE WORK

In this work, we have demonstrated that the application on-line of the divergence criterion for the early warning detection of runaway initiation is feasible. Furthermore, we have shown the equivalence, considering an embedding dimension of one, between Hub and Jones (1987) and  $div>0$  criteria. The use of an embedding dimension of two can be seen as a way to solve the problem of false alarms that the Hub and Jones criterion produces, for example for the case of autocatalytic reactions.

Theoretical results have shown that the best results are obtained by considering three temperature trajectories to calculate the evolution of the state space volume. However, experimentally it seems that only one temperature would produce better results. This is due to the fluctuation and noise present in the system, and further research using different experiments and different reactors is necessary to assess which is the best procedure. Of course, from the practical point of view, the use of only one temperature measurement would simplify considerable the real application of the early warning detection device. Real reactors are in principle dishomogeneous and hence it would be interesting to analyse if the same results are obtaining using Computational Fluid Dynamics (CFD) techniques. A detailed study on the effect of fluctuations of either thermodynamic or environmental origin on the ignition in an explosive system was carried out by Nicolis and Baras (1987). They found that if one considers a spatially distributed system in which a zero-order reaction occurs, the fluctuations induce unexpected symmetry –breaking phenomena, which is reflected in a considerable dispersion of the position of the first “hot spot” initiated in the system. Hence, this study confirms our intuitive idea of increasing of temperature inhomogeneities in approaching the runaway event. A preliminary study on the role of considering spatial dishomogeneities during runaway initiation is in preparation (Rudniak *et al.*, 2002)

In order to develop a robust early warning detection system it is now necessary to study the reconstruction in the case of controlled jacket temperature in which the dynamics of the heating/cooling circuits plus the control system have to be taken into account and, finally, to show their feasibility in “realistic” situations, i.e. in industrial plants under normal and abnormal operating conditions. Our research is continuing along these lines.

**Acknowledgements.** This research has been supported by the EU funded project AWARD (Advanced Warning and Runaway Disposal, contract G1RD-CT-2001-00499) in the GROWTH programme of the European Commission. The authors want to acknowledge to J. Lighthart, M. A. Alós, and H. Nieman for their collaboration during the experiments. Furthermore, the authors gratefully acknowledge the use of the TISEAN programs (Hegger *et al.*, 1999) which has been made generously publicly available at <http://www.mpipks-dresden.mpg.de/~tisean>. The distribution includes an on-line documentation.

## APPENDIX 1. Relationship between the Jacobian in continuous and discrete systems

Let us assume a two-dimensional system given by:

$$\dot{x}(t) = \mathbf{F}(x(t)) \quad (\text{A1})$$

where  $\mathbf{F}=[F_1, F_2]$  and  $x=[x_1, x_2]$ . It is possible to write the linearised version as:

$$\begin{bmatrix} \frac{dy_1}{dt} \\ \frac{dy_2}{dt} \end{bmatrix} = \mathbf{J}(t) \begin{bmatrix} y_1(t) \\ y_2(t) \end{bmatrix} \quad (\text{A2})$$

where  $y_i(t) = \delta x_i(t)$  and  $\mathbf{J}(t)$  is the Jacobian matrix defined by:

$$\mathbf{J}(t) = \begin{bmatrix} j_{11} & j_{12} \\ j_{21} & j_{22} \end{bmatrix} = \begin{bmatrix} \frac{\partial F_1}{\partial x_1} & \frac{\partial F_1}{\partial x_2} \\ \frac{\partial F_2}{\partial x_1} & \frac{\partial F_2}{\partial x_2} \end{bmatrix} \quad (\text{A3})$$

How is the Jacobian for the correspondent discrete system? Let us consider a finite time interval,  $\Delta t$ , the Eq. (A2) reads:

$$\frac{y_1(t + \Delta t) - y_1(t)}{\Delta t} = j_{11} \cdot y_1(t) + j_{12} \cdot y_2(t)$$

$$\frac{y_2(t + \Delta t) - y_2(t)}{\Delta t} = j_{21} \cdot y_1(t) + j_{22} \cdot y_2(t)$$

and, hence:

$$y_1(t + \Delta t) = [j_{11} \cdot \Delta t + 1]y_1(t) + j_{12} \cdot \Delta t \cdot y_2(t)$$

$$y_2(t + \Delta t) = j_{21} \cdot \Delta t \cdot y_1(t) + [j_{22} \cdot \Delta t + 1]y_2(t)$$

which can be grouped as;

$$\begin{bmatrix} y_1(t + \Delta t) \\ y_2(t + \Delta t) \end{bmatrix} = (\mathbf{J}(t) + \mathbf{I}) \begin{bmatrix} y_1(t) \\ y_2(t) \end{bmatrix} \quad (\text{A4})$$

where  $\mathbf{I}$  is the unitary matrix.

## NOTATION

$C_p$	Specific heat capacity
$E$	activation energy
$f_j$	$\exp[\gamma_j(\theta-1)/\theta]$
$k$	reaction rate constant
$n$	reaction order
$S_v$	exchange surface area per unit volume, $m^{-1}$
$T$	Reactor temperature
$T_w$	Jacket temperature, K
$t$	dimensionless time, $k_1(T_w)C_{A_i}^{(n_i-1)}\tau$
$u_A$	dimensionless concentration, $C_A/C_{A_i}$
$U$	Overall heat transfer coefficient, $W/m^2\cdot K$
$z$	conversion, $(1-u)$

## Greek symbols

$\alpha$	dimensionless heat of reaction parameter, $\frac{(-\Delta H_1)C_{A_i}}{\rho_f C_p T_w}$
$\beta$	dimensionless heat transfer parameter, $\frac{US_v}{\rho_f C_p k_1(T_w)C_{A_i}^{(n_i-1)}}$
$\Delta H_i$	heat of the $i$ -th reaction, J/mol
$\gamma_i$	dimensionless activation energy, $\frac{E_i}{RT_w}$
$\lambda_j$	heat of reaction ratio, $\Delta H_j/\Delta H_1$
$\theta$	dimensionless temperature, $\theta = T/T_w$
$\rho_f$	density, $Kg/m^3$
$\rho_j$	reaction rate constant ratio, $\frac{C_{A_i}^{(n_j-n_i)}k_j(T_w)}{k_1(T_w)}$
$\tau$	time, s

## REFERENCES

- Abarbanel, H. D. I., *Analysis of Observed Chaotic Data*, New York, Springer, 1996.
- Adler, J. and Enig, J. W., 1964, The Critical Conditions in Thermal Explosion Theory with Reactant Consumption, *Combust. Flame*, **8**, 97-103.
- Alós, M. A., Nomen, R., Sempere, J., Strozzi, F. and Zaldívar, J. M., 1998, Generalised criteria for boundary safe conditions in semi-batch processes: Simulated and experimental results. *Chem. Engng. Process.* **37**, 405-421.
- Arnold, V. I., 1973, *Ordinary differential equations*, MIT Press, Cambridge.
- Breeden, J. L. and Packard, N. H., 1994, A learning algorithm for optimal representation of experimental data. *Int. J. Bifurcations and Chaos* **4**, 311-
- Broomhead, D. S. and King, G. P., 1986, Extracting qualitative dynamics from experimental data. *Physica D* **20**, 217-236.
- Burden, R. L. and Faires, J. D., 1996, *Numerical Analysis*, 3<sup>rd</sup> Edition, PWS, Boston
- Casdagli, M., Eubank, S., Farmer, J. D., Gibson, J., 1991, State space reconstruction in the presence of noise. *Physica D* **51**, 52-
- Cao, L., 1997, Practical method for determining the minimum embedding dimension of a scalar time series. *Physica D* **110**, 43-50.
- Davies, M., 1994, Noise reduction schemes for chaotic time series. *Physica D* **79**, 174-192
- Diks, C., 1999, *Nonlinear time series analysis: Methods and applications*. World Scientific, Singapore.
- Eckman, J.-P. and Ruelle, D., 1985, Ergodic theory of chaos. *Rev. Mod. Phys.* **57**, 617-656.
- Fraser, A. and Swinney, H., 1986, Independent coordinates for strange attractors from mutual information. *Phys. Rev. A* **33**, 1134-1140.
- Galván, I. M., Zaldívar, J. M., Hernández, H. and Molga, E., 1996, The use of neural networks for fitting complex kinetic data, *Computers Chem. Engng* **20**, 1451-1465.
- Goodwin, G. C. and Sin, K. S., *Adaptive filtering prediction and control*. Prentice-Hall, Englewood Cliffs, 1984.
- Grassberger, P., Hegger, R., Kantz, H., Schaffrath, C and Schreiber, T., 1993, On noise reduction methods for chaotic data, *CHAOS* **3**, 127-141.
- Grassberger, P., Schreiber, T., Schaffrath, C., 1991, Nonlinear time sequence analysis, *Int. J. Bifur. Chaos* **1**, 521-547.
- Haykin, S., *Adaptive filter theory*. Prentice-Hall, Englewood Cliffs, 1991.

- Hegger, R., Kantz, H and Matassini, L., 2000, Denoising human speech signals using chaoslike features. *Phys. Rev. Lett.* **84**, 3197-3200.
- Hegger, R., Kantz, H. and Schreiber, 1999, Practical implementation of nonlinear time series methods: the TISEAN package, *CHAOS* **9**, 413-.
- Hegger, R., Kantz, H. and Schreiber, T., 2002, Nonlinear noise reduction, in *Modelling and Forecasting financial data: Techniques of nonlinear dynamics*, Soofi, A. S. and Cao, L. (eds.), Kluwer, Boston, pp 401-416.
- Hub, L. and Jones, J. D., 1986, Early On-line Detection of Exothermic Reactions, *Plant/Operation Progress*, **5**, 221.
- Isermann, R., 1994, Process fault detection based on modelling and estimation methods- A survey, *Automatica*, **20**, 387.
- Kantz, H. and Schreiber, T., *Nonlinear Time Series Analysis*, Cambridge, Cambridge University Press, 1997.
- Kennel, M. B., Brown, R. and Abarbanel, H. D. I., 1992, Determining embedding dimension for phase-space reconstruction using a geometrical construction. *Phys. Rev. A* **45**, 3403-3411.
- Kostelich, E. J. and Schreiber, T., 1993, Noise reduction in chaotic time-series data: A survey of common methods. *Phys. Rev. E* **48**, 1752-1763.
- Mees, A. I., Rapp, P. E. and Jennings L. S., 1987, Singular value decomposition and embedding dimension. *Phys. Rev. A* **36**, 340-346.
- Nicolis, G. and Baras, F., 1987, Intrinsic randomness and spontaneous symmetry-breaking in explosive systems. *J. of Statistical Physics* **48**, 1071-1090.
- Oppenheim A. V. and Schafer, R. W., *Digital signal processing*, Prentice-Hall, London.1975.
- Packard, N., Crutchfield, J., Farmer, D. and Shaw, R., 1980, Geometry from a time series. *Phys. Rev. Lett.* **45**, 712-715.
- Press, W. H., Flannery, B. P., Teukolsky, S. A., Vetterling, W. T., *Numerical recipes*, Cambridge University Press, Cambridge, 1986.
- Rudniak, L., Strozzi, F., Molga, E. and Zaldívar J. M., 2002, Application of CFD techniques for runaway prediction in chemical reactors (in preparation).
- Sauer, T., Yorke, Y and Casdagli, M., 1991, Embedology, *J. Stat. Phys.* **65**, 579-616.
- Snee, T. J., Barcons, C., Hernández, H. and Zaldívar J.M., 1992, Characterisation of an exothermic reaction using adiabatic and isothermal calorimetry, *J. of Thermal Analysis* **38**, 2729-2747.

- Steensma M. and Westerterp, K. R., 1990, Thermally safe operation of a semi-batch reactor for liquid-liquid reactions. *Ind. Eng. Chem. Res.* **29**, 1259-1270.
- Strozzi, F., 1997, Runaway prevention in chemical reactors using chaos theory techniques. PhD Thesis, Twente University, Twente, The Netherlands.
- Strozzi, F., Zaldívar, J. M., Alós, M. A., and Westerterp, K. R., Towards on-line runaway prevention in chemical reactors using chaos theory techniques. *Procc. of the 9th International Symposium on Loss Prevention and Safety Promotion in the Process Industries*, Barcelona, 4-7 May 1998, pp. 708 -717.
- Strozzi, F., Zaldívar, J. M., Kronberg, A. and Westerterp, K. R., 1999, On-line runaway prevention in chemical reactors using chaos theory techniques. *AIChE J.* **45**, 2429-2443.
- Schreiber, T. and Richter M., 1999, Fast nonlinear projective filtering in a data stream, *Int. J. Bifur. Chaos* **9**, 2039-2045.
- Takens, F., 1981, in *Dynamical Systems and Turbulence*, Warwick 1980, vol 898 of Lecture Notes in Mathematics, edited by A. Rand and L.S. Young, Springer, Berlin, pp 366-381.
- Teman, R., 1997, *Infinite-dimensional dynamical systems in physics and mechanics*, 2<sup>nd</sup> Edition, Springer-Verlag, New York.
- Treichler, J. R., Johnson, C. R. Jr., Larimore, M. G., *Theory and design of adaptive filters*. Wiley, New York, 1987.
- Trulla, L.L, A. Giuliani, J.P. Zbilut, and C.L. Webber, Jr. (1996). Recurrence quantification analysis of the logistic equation with transients. *Phys. Lett. A* **223**, 255-26.
- Varma, A., Morbidelli, M. and Wu, H., *Parametric Sensitivity in Chemical Systems*, Cambridge, Cambridge University Press, 1999.
- Webber Jr. C. L. and Zbilut, J. P., 1994, Dynamical assessment of physiological systems and states using recurrence plot strategies. *J. Appl. Physiol.* **76**, 965-973.
- Zaldívar J.M., Hernández H., Nieman H., Molga E. and Bassani C., 1993, The FIRES project: experimental study of thermal runaway due to agitation problems during toluene nitration, *J. Loss Prev. Process Ind.* **6**, 319-326.
- Zaldívar, J. M., Cano, J., Alós, M. A., Sempere, J., Nomen, R., Lister, D., Maschio, G., Obertopp, T., Gilles, E. D., Bosch, J., and Strozzi, F., 2002, A general criterion to define runaway limits in chemical reactors. *Chemical Engineering Science* (submitted).

Zaldívar, J. M., Hernández, H. and Barcons, C., 1996, Development of a mathematical model and a simulator for the analysis and optimisation of batch reactors: Experimental model characterisation using a reaction calorimeter. *Thermochimica Acta* **289**, 267-302.

Zbilut, J. P., Zaldívar, J. M., and Strozzi, F., 2002, Recurrence quantification based-liapunov exponents for monitoring divergence in experimental data. *Phys. Lett. A* **297**, 173-181.





## **Mission of the JRC**

The mission of the JRC is to provide customer-driven scientific and technical support for the conception, development, implementation and monitoring of EU policies. As a service of the European Commission, the JRC functions as a reference centre of science and technology for the Union. Close to the policy-making process, it serves the common interest of the Member States, while being independent of special interests, whether private or national.



EUROPEAN COMMISSION  
JOINT RESEARCH CENTRE